

## 5 Leptonic and semileptonic kaon and pion decay and $|V_{ud}|$ and $|V_{us}|$

Authors: T. Kaneko, J. N. Simone, N. Tantalo

This section summarizes state-of-the-art lattice calculations of the leptonic kaon and pion decay constants,  $f_K^\pm$  and  $f_\pi^\pm$ , and the kaon semileptonic-decay form factor  $f_+(0)$ , and provides an analysis in the framework of the Standard Model. With respect to the previous edition of the FLAG review [1], there has been a new study each for the decay constants and  $f_+(0)$  for  $N_f = 2 + 1$ , and a new entry to the average of the ratio  $f_{K^\pm}/f_{\pi^\pm}$  for  $N_f = 2 + 1 + 1$ .<sup>1</sup> As in Ref. [1], when combining lattice data with experimental results, we take into account the strong isospin correction, either obtained in lattice calculations or estimated by using chiral perturbation theory ( $\chi$ Pt), both for  $f_{K^\pm}$  and  $f_{K^\pm}/f_{\pi^\pm}$ .

### 5.1 Experimental information concerning $|V_{ud}|$ , $|V_{us}|$ , $f_+(0)$ and $f_{K^\pm}/f_{\pi^\pm}$

The following review relies on the fact that precision experimental data on kaon decays very accurately determine the product  $|V_{us}|f_+(0)$  [3] and the ratio  $|V_{us}/V_{ud}|f_{K^\pm}/f_{\pi^\pm}$  [3, 4]:

$$|V_{us}|f_+(0) = 0.21654(41), \quad \left| \frac{V_{us}}{V_{ud}} \right| \frac{f_{K^\pm}}{f_{\pi^\pm}} = 0.27599(41). \quad (65)$$

Here, and in the following,  $f_{K^\pm}$  and  $f_{\pi^\pm}$  are the isospin-broken decay constants in QCD. We will refer to the decay constants in the isospin-symmetric limit as  $f_K$  and  $f_\pi$  (the latter at leading order in the mass difference  $(m_u - m_d)$  coincides with  $f_{\pi^\pm}$ ). The parameters  $|V_{ud}|$  and  $|V_{us}|$  are elements of the Cabibbo-Kobayashi-Maskawa matrix and  $f_+(q^2)$  represents one of the form factors relevant for the semileptonic decay  $K^0 \rightarrow \pi^- \ell \nu$ , which depends on the momentum transfer  $q$  between the two mesons. What matters here is the value at  $q^2 = 0$ :

$$f_+(0) \equiv f_+^{K^0 \pi^-}(0) = f_0^{K^0 \pi^-}(0) = q^\mu \langle \pi^-(p') | \bar{s} \gamma_\mu u | K^0(p) \rangle / (M_K^2 - M_\pi^2) \Big|_{q^2 \rightarrow 0}. \quad (66)$$

The pion and kaon decay constants are defined by<sup>2</sup>

$$\langle 0 | \bar{d} \gamma_\mu \gamma_5 u | \pi^+(p) \rangle = i p_\mu f_{\pi^+}, \quad \langle 0 | \bar{s} \gamma_\mu \gamma_5 u | K^+(p) \rangle = i p_\mu f_{K^+}. \quad (67)$$

In this normalization,  $f_{\pi^\pm} \simeq 130$  MeV,  $f_{K^\pm} \simeq 155$  MeV.

In Eq. (65), the electromagnetic effects have already been subtracted in the experimental analysis using  $\chi$ Pt [11–14]. In 2015, a new method [15] has been proposed by the RM123-SOTON collaboration for calculating the leptonic decay rates of hadrons including both QCD and QED on the lattice, and successfully applied to the case of the ratio of the leptonic decay

<sup>1</sup>In this edition, we omit results for  $N_f = 2$ , because there has been no new entry after 2014. We refer to the 2016 edition [2] for the  $N_f = 2$  results.

<sup>2</sup>The pion decay constant represents a QCD matrix element—in the full Standard Model, the one-pion state is not a meaningful notion: the correlation function of the charged axial current does not have a pole at  $p^2 = M_{\pi^+}^2$ , but a branch cut extending from  $M_{\pi^+}^2$  to  $\infty$ . The analytic properties of the correlation function and the problems encountered in the determination of  $f_\pi$  are thoroughly discussed in Ref. [5]. The “experimental” value of  $f_\pi$  depends on the convention used when splitting the sum  $\mathcal{L}_{\text{QCD}} + \mathcal{L}_{\text{QED}}$  into two parts. The lattice determinations of  $f_\pi$  do not yet reach the accuracy where this is of significance, but at the precision claimed by the Particle Data Group [6, 7], the numerical value does depend on the convention used [5, 8–10].

rates of kaons and pions [16, 17]. By employing the twisted-mass discretization, they simulate  $N_f = 2 + 1 + 1$  QCD at three lattice spacings  $a = 0.07, 0.08, 0.09$  fm with pion masses down to  $\approx 220$  MeV on multiple lattice volumes to directly examine finite-volume effects. The correction to the  $K_{\mu 2}/\pi_{\mu 2}$  decay rate, including both electromagnetic and strong isospin-breaking effects, is found to be equal to  $-1.26(14)\%$  [17] to be compared to the estimate  $-1.12(21)\%$  based on  $\chi$ PT [14, 18].<sup>3</sup> Using the experimental values of the  $K_{\mu 2}$  and  $\pi_{\mu 2}$  decay rates the result of Ref. [17] implies

$$\left| \frac{V_{us}}{V_{ud}} \right| \frac{f_K}{f_\pi} = 0.27683(29)_{\text{exp}}(20)_{\text{th}} [35], \quad (68)$$

where the last error in brackets is the sum in quadrature of the experimental and theoretical uncertainties, and the ratio of the decay constants is the one corresponding to isosymmetric QCD. A large part of the theoretical uncertainty comes from the statistical error and continuum and chiral extrapolation of lattice data, which can be systematically reduced by a more realistic simulation with high statistics.

An independent study of the electromagnetic effects is carried out by the RBC/UKQCD collaboration using the domain-wall discretization [19]. They simulate  $N_f = 2 + 1$  QCD at a single lattice spacing  $a = 0.11$  fm, a pion mass close to its physical value, and a lattice volume with  $M_\pi L \sim 3.9$ . Their result  $-0.86(_{-40}^{+41})\%$  including the strong isospin corrections is consistent with the RM123-SOTON estimate. The larger uncertainty is due to the possibly large finite-volume effects, which are under active investigation in different lattice-QED prescriptions [20].

At present, the superallowed nuclear  $\beta$  transitions provide the most precise determination of  $|V_{ud}|$ . Its accuracy has been limited by hadronic uncertainties in the universal electroweak radiative correction  $\Delta_R^V$ . A 2018 analysis in terms of a dispersion relation [21, 22] found  $\Delta_R^V$  larger than the previous estimate [23]. A more straightforward update [24] of Ref. [23] on the description of relevant hadronic contributions as well as a lattice and perturbative-QCD calculation [25] also reported larger  $\Delta_R^V$ , which is consistent with the dispersive estimate within uncertainties. Together with conservative estimate of nuclear corrections [21, 26–34], a recent reanalysis of twenty-three  $\beta$  decays obtained [4, 35]

$$|V_{ud}| = 0.97373(31). \quad (69)$$

The matrix element  $|V_{us}|$  can be determined from inclusive hadronic  $\tau$  decays [36–39]. Both Gamiz *et al.* [40, 41] and Maltman *et al.* [38, 42, 43] arrived at very similar values of  $|V_{us}|$  by separating the inclusive decay  $\tau \rightarrow X_{\{d,s\}}\nu_\tau$  into nonstrange ( $X_d\nu_\tau$ ) and strange ( $X_s\nu_\tau$ ) final states and evaluating the relevant spectral integral using the operator product expansion (OPE). However,  $|V_{us}| = 0.2195(19)$  quoted by HFLAV 18 [44] differs from the result one obtains from the kaon decays by about three standard deviations (see Tab. 20 in Sec. 5.5). A new treatment of higher orders in the OPE obtained a slightly larger value of  $|V_{us}| = 0.2219(22)$  with a different experimental input [45].

Reference [46] proposed a new method to determine  $|V_{us}|$  without any recourse to the OPE by evaluating the spectral integral from lattice-QCD data of the hadronic vacuum polarization function through generalized dispersion relations. This led to an analysis [45] yielding  $|V_{us}| = 0.2240(18)$ , which is consistent with that from the kaon decays. However,

<sup>3</sup>See the discussion concerning the definition of QCD and of the isospin-breaking corrections in Sec. 3.

this result mostly relies on the  $\tau \rightarrow K\nu_\tau$  decay channel, which represents only  $\sim 24\%$  of the inclusive  $\tau \rightarrow X_s\nu_\tau$  decay, due to their choice of the generalized dispersion relation [47].

The ETM collaboration carried out a first lattice calculation of the *fully* inclusive rate of the hadronic  $\tau$  decays based on ideas to study inclusive processes on the lattice [48, 49]. Their study of  $\tau \rightarrow X_d\nu_\tau$  led to 0.4% determination of  $|V_{ud}| = 0.9752(39)$ , which is nicely consistent with Eq. (69) from nuclear  $\beta$  decay [50]. Their extension to the  $\tau \rightarrow X_s\nu_\tau$  decay yields  $|V_{us}| = 0.2189(19)$  and confirms the above tension with that from the kaon decays [51]. In Sec. 5.5 of this review, we quote

$$|V_{us}| = 0.2184(21) \quad (70)$$

from HFLAV 22 [52] as  $|V_{us}|$  from the inclusive hadronic  $\tau$  decays.

The experimental results in Eq. (65) are for the semileptonic decay of a neutral kaon into a negatively charged pion and the charged pion and kaon leptonic decays, respectively, in QCD. In the case of the semileptonic decays the corrections for strong and electromagnetic isospin breaking in  $\chi$ PT at NLO have allowed for averaging the different experimentally measured isospin channels [53]. This is quite a convenient procedure as long as lattice-QCD calculations do not include strong or QED isospin-breaking effects. Several lattice results for  $f_K/f_\pi$  are quoted for QCD with (squared) pion and kaon masses of  $M_\pi^2 = M_{\pi^0}^2$  and  $M_K^2 = \frac{1}{2}(M_{K^\pm}^2 + M_{K^0}^2 - M_{\pi^\pm}^2 + M_{\pi^0}^2)$  for which the leading strong and electromagnetic isospin violations cancel. For these results, contact with experimental results is made by correcting leading isospin breaking guided either by  $\chi$ PT or by lattice calculations. We note, however, that the modern trend for the leptonic decays is to include strong and electromagnetic isospin breaking in the lattice calculations (e.g., Refs. [15, 16, 54–60]).

This trend is being extended to the semileptonic decays. Calculating the electromagnetic correction to the  $K_{\ell 3}$  semileptonic decays on the lattice is more involved due to the photon exchange between  $\pi^\pm$  and  $\ell^\mp$  in the final state. A framework has been proposed [61], and its applicability to the kaon semileptonic decays has been discussed in Ref. [62]. References [63–65] pursue an effective field theory setup supplemented by nonperturbative lattice-QCD inputs to estimate the radiative corrections.

## 5.2 Lattice results for $f_+(0)$ and $f_{K^\pm}/f_{\pi^\pm}$

The traditional way of determining  $|V_{us}|$  relies on using estimates for the value of  $f_+(0)$ , invoking the Ademollo-Gatto theorem [66]. This theorem states that the corrections to the SU(3) symmetric limit  $f_+(0) = 1$  start at second order in SU(3) breaking, namely  $\propto (m_s - m_{ud})^2$ . Theoretical models are used to estimate higher-order corrections. Lattice methods have now reached the stage where quantities like  $f_+(0)$  or  $f_K/f_\pi$  can be determined to good accuracy. As a consequence, the uncertainties inherent in the theoretical estimates for the higher order effects in the value of  $f_+(0)$  do not represent a limiting factor any more, and we shall, therefore, not invoke those estimates. Also, we will use the experimental results based on nuclear  $\beta$  decay and inclusive hadronic  $\tau$  decay exclusively for comparison—the main aim of the present review is to assess the information gathered with lattice methods and to use it for testing the consistency of the SM and its potential to provide constraints for its extensions.

The database underlying the present review of the semileptonic form factor and the ratio of decay constants is listed in Tabs. 16 and 17. The properties of the lattice data play a crucial role for the conclusions to be drawn from these results: ranges of  $a$ ,  $M_\pi$  and  $LM_\pi$  to control continuum extrapolation, extrapolation in the quark masses, finite-size effects,

etc. The key features of the various data sets are characterized by means of the colour code specified in Sec. 2.1. More detailed information on individual computations are compiled in Appendix C.2, which in this edition is limited to new results and to those entering the FLAG averages. For other calculations the reader should refer to the Appendix B.2 of Ref. [2].

The quantity  $f_+(0)$  represents a matrix element of a strangeness-changing null-plane charge,  $f_+(0) = \langle K|Q^{\bar{u}s}|\pi\rangle$  (see Ref. [67]). The vector charges obey the commutation relations of the Lie algebra of SU(3), in particular  $[Q^{\bar{u}s}, Q^{\bar{s}u}] = Q^{\bar{u}u-\bar{s}s}$ . This relation implies the sum rule  $\sum_n |\langle K|Q^{\bar{u}s}|n\rangle|^2 - \sum_n |\langle K|Q^{\bar{s}u}|n\rangle|^2 = 1$ . Since the contribution from the one-pion intermediate state to the first sum is given by  $f_+(0)^2$ , the relation amounts to an exact representation for this quantity [68]:

$$f_+(0)^2 = 1 - \sum_{n \neq \pi} |\langle K|Q^{\bar{u}s}|n\rangle|^2 + \sum_n |\langle K|Q^{\bar{s}u}|n\rangle|^2. \quad (71)$$

While the first sum on the right extends over nonstrange intermediate states, the second runs over exotic states with strangeness  $\pm 2$  and is expected to be small compared to the first.

The expansion of  $f_+(0)$  in SU(3)  $\chi$ PT in powers of  $m_u$ ,  $m_d$ , and  $m_s$  starts with  $f_+(0) = 1 + f_2 + f_4 + \dots$  [69]. The NLO contribution  $f_2$  is known, since it can be expressed in terms of  $M_\pi$ ,  $M_K$ ,  $M_\eta$  and  $f_\pi$  [67]. In the language of the sum rule (71),  $f_2$  stems from nonstrange intermediate states with three mesons. Like all other nonexotic intermediate states, it lowers the value of  $f_+(0)$ :  $f_2 = -0.023$  when using the experimental value of  $f_\pi$  as input. The corresponding expressions have also been derived in quenched or partially quenched (staggered)  $\chi$ PT [70, 71]. At the same order in the SU(2) expansion [72],  $f_+(0)$  is parameterized in terms of  $M_\pi$  and two *a priori* unknown parameters. The latter can be determined from the dependence of the lattice results on the masses of the quarks. For the SU(3)  $\chi$ PT formula for  $f_2$ , one may use  $f_0$ , that is the decay constant in the chiral limit, instead of  $f_\pi$ . While this affects the result only at higher orders, it may make a significant numerical difference in calculations where the higher-order corrections are not explicitly accounted for. (Lattice results concerning the value of the ratio  $f_\pi/f_0$  are reviewed in Sec. 5.3 of the previous review [1].)

The lattice results shown in Fig. 8 indicate that the higher order contributions  $\Delta f \equiv f_+(0) - 1 - f_2$  are negative and thus amplify the effect generated by  $f_2$ . This confirms the expectation that the exotic contributions are small. The entries in the lower part represent various model estimates for  $f_4$ . In Ref. [73], the symmetry-breaking effects are estimated in the framework of the quark model. The more recent calculations are more sophisticated, as they make use of the known explicit expression for the  $K_{\ell 3}$  form factors to NNLO in  $\chi$ PT [74, 75]. The corresponding formula for  $f_4$  accounts for the chiral logarithms occurring at NNLO and is not subject to the ambiguity mentioned above.<sup>4</sup> The numerical result, however, depends on the model used to estimate the low-energy constants occurring in  $f_4$  [75–78]. The figure indicates that the most recent numbers obtained in this way correspond to a positive or an almost vanishing rather than a negative value for  $\Delta f$ . We note that FNAL/MILC 12I [71], JLQCD 17 [79], FNAL/MILC 18 [80], and Ref. [81] have made an attempt at determining a combination of some of the low-energy constants appearing in  $f_4$  from lattice data.

<sup>4</sup>Fortran programs for the numerical evaluation of the form factor representation in Ref. [75] are available on request from Johan Bijnens.

### 5.3 Direct determination of $f_+(0)$ and $f_{K^\pm}/f_{\pi^\pm}$

Many lattice results for the form factor  $f_+(0)$  and for the ratio of decay constants, which we summarize here in Tabs. 16 and 17, respectively, have been computed in isospin-symmetric QCD. The reason for this unphysical parameter choice is that there are only a few simulations of isospin-breaking effects in lattice QCD, which is ultimately the cleanest way for predicting these effects [15, 16, 19, 55, 58–60, 82–85]. In the meantime, one relies either on  $\chi$ PT [69, 86] to estimate the correction to the isospin limit or one calculates the breaking at leading order in  $(m_u - m_d)$  in the valence quark sector by extrapolating the lattice data for the charged kaons to the physical value of the  $up(down)$ -quark mass (the result for the pion decay constant is always extrapolated to the value of the average light-quark mass  $\hat{m}$ ). This defines the prediction for  $f_{K^\pm}/f_{\pi^\pm}$ .

Since the majority of results that qualify for inclusion into the FLAG average include the strong isospin-breaking correction, we provide in Fig. 9 the overview of the world data of  $f_{K^\pm}/f_{\pi^\pm}$ . For all the results of Tab. 17 provided only in the isospin-symmetric limit we apply individually an isospin correction that will be described later on (see Eqs. (74)–(75)).

The plots in Figs. 8 and 9 illustrate our compilation of data for  $f_+(0)$  and  $f_{K^\pm}/f_{\pi^\pm}$ . The lattice data for the latter quantity is largely consistent even when comparing simulations with different  $N_f$ . In the case of  $f_+(0)$ , a slight tendency to get higher values when increasing  $N_f$  seems to be visible, while it does not exceed one standard deviation. We now proceed to form the corresponding averages, separately for the data with  $N_f = 2 + 1 + 1$  and  $N_f = 2 + 1$  dynamical flavours, and in the following we will refer to these averages as the “direct” determinations.

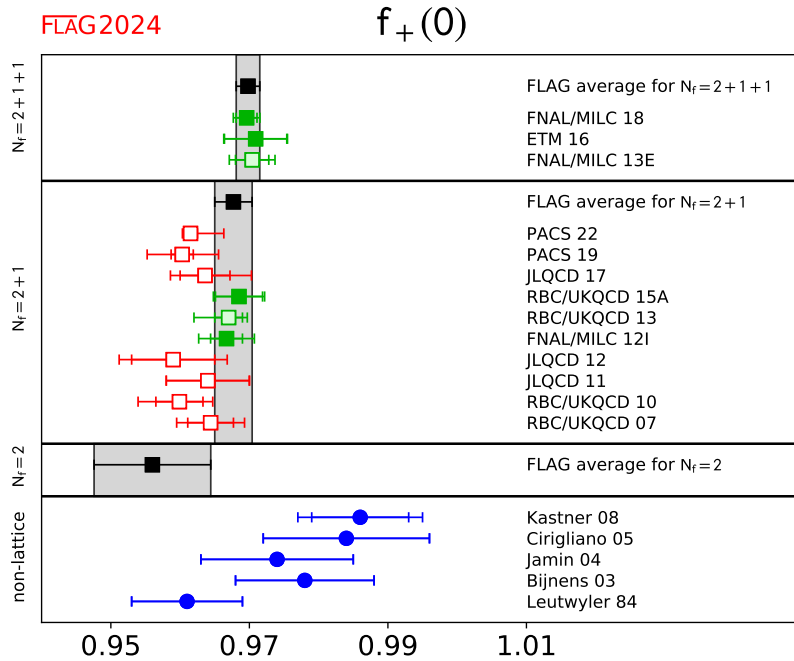


Figure 8: Comparison of lattice results (squares) for  $f_+(0)$  with various model estimates based on  $\chi$ PT [73, 75–78] (blue circles). The black squares and grey bands indicate our averages in Eqs. (72) and (73). The significance of the colours is explained in Sec. 2.

Collaboration	Ref.	$N_f$	publication status	chiral extrapolation	continuum extrapolation	finite-volume errors	$f_+(0)$
FNAL/MILC 18	[80]	2+1+1	A	★	★	★	0.9696(15)(12)
ETM 16	[87]	2+1+1	A	○	★	○	0.9709(45)(9)
FNAL/MILC 13E	[88]	2+1+1	A	★	★	★	0.9704(24)(22)
PACS 22	[89]	2+1	A	○	■	★	0.9615(10)( $^{+47}_{-6}$ )
PACS 19	[90]	2+1	A	○	■	★	0.9603(16)( $^{+50}_{-48}$ )
JLQCD 17	[79]	2+1	A	○	■	○	0.9636(36)( $^{+57}_{-35}$ )
RBC/UKQCD 15A	[91]	2+1	A	★	○	○	0.9685(34)(14)
RBC/UKQCD 13	[92]	2+1	A	★	○	○	0.9670(20)( $^{+18}_{-46}$ )
FNAL/MILC 12I	[71]	2+1	A	○	○	★	0.9667(23)(33)
JLQCD 12	[93]	2+1	C	○	■	★	0.959(6)(5)
JLQCD 11	[94]	2+1	C	○	■	★	0.964(6)
RBC/UKQCD 10	[95]	2+1	A	○	■	★	0.9599(34)( $^{+31}_{-47}$ )(14)
RBC/UKQCD 07	[96]	2+1	A	○	■	★	0.9644(33)(34)(14)

Table 16: Colour codes for the data on  $f_+(0)$ . In this and previous editions [1, 97], old results with two red tags have been dropped.

### 5.3.1 Results for $f_+(0)$

For  $f_+(0)$  there are currently two computational strategies: FNAL/MILC uses the Ward identity to relate the  $K \rightarrow \pi$  form factor at zero momentum transfer to the matrix element  $\langle \pi | S | K \rangle$  of the flavour-changing scalar current  $S = \bar{s}u$ . Peculiarities of the staggered fermion discretization used by FNAL/MILC (see Ref. [71]) makes this the favoured choice. The other collaborations are instead computing the vector current matrix element  $\langle \pi | \bar{s}\gamma_\mu u | K \rangle$ . Apart from FNAL/MILC 13E, RBC/UKQCD 15A, FNAL/MILC 18, PACS 19 and 22, all simulations in Tab. 16 involve unphysically heavy quarks and, therefore, the lattice data needs to be extrapolated to the physical pion and kaon masses corresponding to the  $K^0 \rightarrow \pi^-$  channel. We note also that the recent computations of  $f_+(0)$  make use of the partially-twisted boundary conditions to determine the form-factor results directly at the relevant kinematical point  $q^2 = 0$  [98, 99], avoiding in this way any uncertainty due to the momentum dependence of the vector and/or scalar form factors. The ETM collaboration uses partially-twisted boundary conditions to compare the momentum dependence of the scalar and vector form factors with the one of the experimental data [87, 100], while keeping at the same time the advantage of the high-precision determination of the scalar form factor at the kinematical end-point  $q_{max}^2 = (M_K - M_\pi)^2$  [101, 102] for the interpolation at  $q^2 = 0$ .

According to the colour codes reported in Tab. 16 and to the FLAG rules of Sec. 2.2, the results FNAL/MILC 12I and RBC/UKQCD 15A with  $N_f = 2 + 1$ , and the results ETM 16 and FNAL/MILC 18 with  $N_f = 2 + 1 + 1$  dynamical flavours of fermions, respectively, can enter the FLAG averages. Therefore, there is no new entry to form the averages in Eqs. (72)

and (73) in this edition.

At  $N_f = 2 + 1 + 1$  the result from the FNAL/MILC collaboration,  $f_+(0) = 0.9704(24)(22)$  (FNAL/MILC 13E), is based on the use of the Highly Improved Staggered Quark (HISQ) action (for both valence and sea quarks), which has been tailored to reduce staggered taste-breaking effects, and includes simulations with three lattice spacings and physical light-quark masses. These features lead to uncertainties due to the chiral extrapolation and the discretization artifacts that are well below the statistical error. The remaining largest systematic uncertainty comes from finite-size effects, which have been investigated in Ref. [103] using one-loop  $\chi$ PT (with and without taste-violating effects). In Ref. [80], the FNAL/MILC collaboration presented a more precise determination of  $f_+(0)$ ,  $f_+(0) = 0.9696(15)(11)$  (FNAL/MILC 18). In this update, their analysis is extended to two smaller lattice spacings  $a = 0.06$  and  $0.042$  fm. The physical light-quark mass is simulated at four lattice spacings. They also added a simulation at a small volume to study the finite-size effects. The improvement of the precision with respect to FNAL/MILC 13E is obtained mainly by an estimate of finite-size effects, which is claimed to be controlled at the level of  $\sim 0.05\%$  by comparing two analyses with and without the one-loop correction. The total uncertainty is reduced to  $\sim 0.2\%$ . An independent calculation of such high precision would be highly welcome to solidify the lattice prediction of  $f_+(0)$ , which currently suggests a tension with CKM unitarity with the updated value of  $|V_{ud}|$  (see Sec. 5.4).

The result from the ETM collaboration,  $f_+(0) = 0.9709(45)(9)$  (ETM 16), makes use of the twisted-mass discretization adopting three values of the lattice spacing in the range  $0.06$ – $0.09$  fm and pion masses simulated in the range  $210$ – $450$  MeV. The chiral and continuum extrapolations are performed in a combined fit together with the momentum dependence, using both a  $SU(2)$ - $\chi$ PT inspired ansatz (following Ref. [100]) and a modified  $z$ -expansion fit. The uncertainties coming from the chiral extrapolation, the continuum extrapolation and the finite-volume effects turn out to be well below the dominant statistical error, which includes also the error due to the fitting procedure. A set of synthetic data points, representing both the vector and the scalar semileptonic form factors at the physical point for several selected values of  $q^2$ , is provided together with the corresponding correlation matrix.

In ETM 16, a measure of the scaling violation  $\delta(a)$  defined in Eq. (1) estimated from their continuum and chiral extrapolation decreases toward the chiral limit with the strange-quark mass kept fixed, because the  $SU(3)$ -breaking effects to be calculated on the lattice increases, and more statistics are needed to keep the statistical accuracy toward this limit. At the physical point,  $\delta(a)$  is consistent with zero in their region of the lattice spacing  $a$ . This is also the case for FNAL/MILC 18, where they demonstrated that  $f_+(0)$  extrapolated to the physical point at each simulated value of  $a$  is consistent with the value extrapolated to the continuum limit within  $2\sigma$ . We note that, in contrast to the heavy-meson semileptonic decays, relevant meson masses and momenta at zero momentum transfer are at most  $\mathcal{O}(M_K)$ , and hence well below the cutoff  $a^{-1}$ .

The PACS collaboration carried out a calculation (PACS 19) for  $N_f = 2 + 1$  using the  $\mathcal{O}(a)$ -improved Wilson quark action by creating an ensemble with the physical light-quark mass on a large lattice volume of  $(10.9 \text{ fm})^4$  at a single spacing  $a = 0.085$  fm [90]. Such a large lattice enables them to interpolate  $f_+(q^2)$  to zero momentum transfer and study the momentum-transfer dependence of the form factors without using partially-twisted boundary conditions. This was extended to a smaller lattice spacing  $a = 0.063$  fm in PACS 22, which yields  $f_+(0) = 0.9615(10) \left( \begin{smallmatrix} +47 \\ -6 \end{smallmatrix} \right)$ . However, their result does not enter the FLAG average, because they simulate only two lattice spacings using unimproved local and conserved vector

currents. That setup is the source of the largest (and very asymmetric) error in their calculation. Further extension to an even smaller lattice spacing  $a = 0.041$  fm has been reported in Ref. [104], where authors estimate the statistical error only, and refrain from quoting a numerical value of  $f_+(0)$ .

For  $N_f = 2 + 1$ , the two results eligible to enter the FLAG average are the one from RBC/UKQCD 15A,  $f_+(0) = 0.9685(34)(14)$  [91], and the one from FNAL/MILC 12I,  $f_+(0) = 0.9667(23)(33)$  [71]. These results, based on different fermion discretizations (staggered fermions in the case of FNAL/MILC and domain wall fermions in the case of RBC/UKQCD) are in nice agreement. Moreover, in the case of FNAL/MILC the form factor has been determined from the scalar current matrix element, while in the case of RBC/UKQCD it has been determined including also the matrix element of the vector current. To a certain extent, both simulations are expected to be affected by different systematic effects.

RBC/UKQCD 15A has analyzed results on ensembles with pion masses down to 140 MeV, mapping out the complete range from the SU(3)-symmetric limit to the physical point. No significant cut-off effects (results for two lattice spacings) were observed in the simulation results. Ensembles with unphysical light-quark masses are weighted to work as a guide for small corrections toward the physical point, reducing in this way the model dependence in the fitting ansatz. The systematic uncertainty turns out to be dominated by finite-volume effects, for which an estimate based on effective theory arguments is provided.

The result FNAL/MILC 12I is from simulations reaching down to a lightest RMS pion mass of about 380 MeV (the lightest valence pion mass for one of their ensembles is about 260 MeV). Their combined chiral and continuum extrapolation (results for two lattice spacings) is based on NLO staggered  $\chi$ Pt supplemented by the continuum NNLO expression [75] and a phenomenological parameterization of the breaking of the Ademollo-Gatto theorem at finite lattice spacing inherent in their approach. The  $p^4$  low-energy constants entering the NNLO expression have been fixed in terms of external input [105].

Since there has been no new entry after the previous edition, the FLAG average for  $f_+(0)$  remains unchanged. The  $N_f = 2 + 1 + 1$  average is based on the FNAL/MILC 18 and ETM 16 (uncorrelated) results, the  $N_f = 2 + 1$  average based on FNAL/MILC 12I and RBC/UKQCD 15A, which we consider uncorrelated:

$$\text{direct, } N_f = 2 + 1 + 1 : \quad f_+(0) = 0.9698(17) \quad \text{Refs. [80, 87],} \quad (72)$$

$$\text{direct, } N_f = 2 + 1 : \quad f_+(0) = 0.9677(27) \quad \text{Refs. [71, 91].} \quad (73)$$

We stress that the results (72) and (73), corresponding to  $N_f = 2 + 1 + 1$  and  $N_f = 2 + 1$ , respectively, include simulations with physical light-quark masses.

### 5.3.2 Results for $f_{K^\pm}/f_{\pi^\pm}$

In the case of the ratio of decay constants, the data sets that meet the criteria formulated in the introduction are HPQCD 13A [112], ETM 14E [109], FNAL/MILC 17 [108] (which updates FNAL/MILC 14A [110]), CalLat 20 [107] and ETM 21 [106] with  $N_f = 2 + 1 + 1$ , and HPQCD/UKQCD 07 [131], MILC 10 [123], BMW 10 [126], RBC/UKQCD 14B [120], BMW 16 [118, 119], QCDSF/UKQCD 16 [117], and CLQCD 23 [116] with  $N_f = 2 + 1$  dynamical flavours. Note that the new entry in this edition is ETM 21 for  $N_f = 2 + 1 + 1$ , which did not enter the previous FLAG average due to its publication status, and CLQCD 23 for  $N_f = 2 + 1$ .

CalLat 20 employs a mixed action setup with Möbius domain-wall valence quarks on gradient-flowed HISQ ensembles at four lattice spacings  $a = 0.06\text{--}0.15$  fm. The valence pion



Collaboration	Ref.	$N_f$	publication status	chiral extrapolation	continuum extrapolation	finite-volume errors	$f_K/f_\pi$	$f_{K^\pm}/f_{\pi^\pm}$
ETM 21	[106]	2+1+1	A	★	★	★	1.1995(44)(7)	1.1957(44)(7)
CalLat 20	[107]	2+1+1	A	★	★	★	1.1964(32)(30)	1.1942(32)(31)
FNAL/MILC 17	[108]	2+1+1	A	★	★	★	1.1980(12)( $^{+5}_{-15}$ )	1.1950(15)( $^{+6}_{-18}$ )
ETM 14E	[109]	2+1+1	A	○	★	○	1.188(11)(11)	1.184(12)(11)
FNAL/MILC 14A	[110]	2+1+1	A	★	★	★		1.1956(10)( $^{+26}_{-18}$ )
ETM 13F	[111]	2+1+1	C	○	★	○	1.193(13)(10)	1.183(14)(10)
HPQCD 13A	[112]	2+1+1	A	★	○	★	1.1948(15)(18)	1.1916(15)(16)
MILC 13A	[113]	2+1+1	A	★	★	★		1.1947(26)(37)
MILC 11	[114]	2+1+1	C	○	○	○		1.1872(42) $^{\dagger}_{\text{stat.}}$
ETM 10E	[115]	2+1+1	C	○	○	○	1.224(13) $_{\text{stat}}$	
CLQCD 23	[116]	2+1	A	★	★	★		1.1907(76)(17)
QCDSF/UKQCD 16	[117]	2+1	A	○	★	○	1.192(10)(13)	1.190(10)(13)
BMW 16	[118, 119]	2+1	A	★	★	★	1.182(10)(26)	1.178(10)(26)
RBC/UKQCD 14B	[120]	2+1	A	★	★	★	1.1945(45)	
RBC/UKQCD 12	[121]	2+1	A	★	○	★	1.199(12)(14)	
Laiho 11	[122]	2+1	C	○	★	○		1.202(11)(9)(2)(5) $^{\dagger\dagger}$
MILC 10	[123]	2+1	C	○	★	★		1.197(2)( $^{+3}_{-7}$ )
JLQCD/TWQCD 10	[124]	2+1	C	○	■	★	1.230(19)	
RBC/UKQCD 10A	[125]	2+1	A	○	○	★	1.204(7)(25)	
BMW 10	[126]	2+1	A	★	★	★	1.192(7)(6)	
MILC 09A	[127]	2+1	C	○	★	★		1.198(2)( $^{+6}_{-8}$ )
MILC 09	[128]	2+1	A	○	★	★		1.197(3)( $^{+6}_{-13}$ )
Aubin 08	[129]	2+1	C	○	○	○		1.191(16)(17)
RBC/UKQCD 08	[130]	2+1	A	○	■	★	1.205(18)(62)	
HPQCD/UKQCD 07	[131]	2+1	A	○	○	○	1.189(2)(7)	
MILC 04	[86]	2+1	A	○	○	○		1.210(4)(13)

$^{\dagger}$  Result with statistical error only from polynomial interpolation to the physical point.

$^{\dagger\dagger}$  This work is the continuation of Aubin 08.

Table 17: Colour codes for the data on the ratio of decay constants:  $f_K/f_\pi$  is the pure QCD isospin-symmetric ratio, while  $f_{K^\pm}/f_{\pi^\pm}$  is in pure QCD including the isospin-breaking correction. In this and previous editions [1, 97], old results with two red tags have been dropped.

mass reaches the physical point at three lattice spacings, and the smallest valence-sea and sea pion masses are below 200 MeV. Finite-volume corrections are studied on three lattice volumes at  $a = 0.12$  fm and  $M_\pi \sim 220$  MeV. The extrapolation to the continuum limit and the physical point is based on NNLO  $\chi$ PT [132]. A comprehensive study of systematic uncertainties is performed by exploring several options including the use of the mixed-action effective theory expression, and the inclusion of N<sup>3</sup>LO counter terms. They obtain  $f_{K^\pm}/f_{\pi^\pm} = 1.1942(32)_{\text{stat}}(12)_\chi(20)_{a^2}(1)_{FV}(12)_M(7)_{IB}$ , where the errors are statistical, due

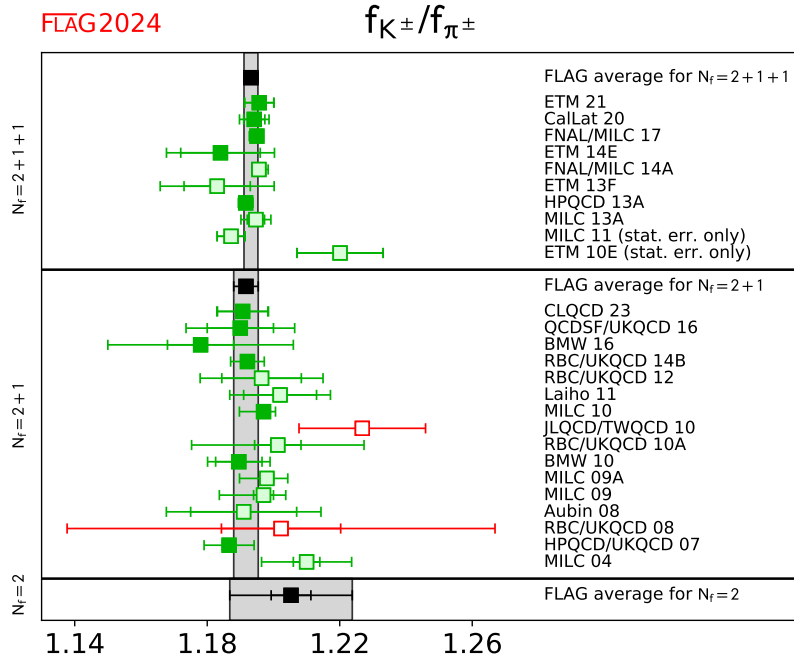


Figure 9: Comparison of lattice results for  $f_{K^\pm}/f_{\pi^\pm}$ . This ratio is obtained in pure QCD including the isospin-breaking correction (see Sec. 5.3). The black squares and grey bands indicate our averages in Eqs. (76) and (77).

to the extrapolation in pion and kaon masses, extrapolation in  $a^2$ , finite-size effects, choice of the fitting form and strong isospin-breaking corrections.

ETM 14E uses the twisted-mass discretization and provides a comprehensive study of the systematics by presenting results for three lattice spacings in the range 0.06–0.09 fm and for pion masses in the range 210–450 MeV. This makes it possible to constrain the chiral extrapolation, using both SU(2) [72]  $\chi$ PT and polynomial fits. The ETM collaboration includes the spread in the central values obtained from different ansätze into the systematic errors. The final result of their analysis is  $f_{K^\pm}/f_{\pi^\pm} = 1.184(12)_{\text{stat+fit}}(3)_{\text{Chiral}}(9)_{a^2}(1)_{Z_P}(3)_{FV}(3)_{IB}$  where the errors are (statistical + the error due to the fitting procedure), due to the chiral extrapolation, the continuum extrapolation, the mass-renormalization constant, the finite-volume and (strong) isospin-breaking effects.

In ETM 21 [106], the ETM collaboration presented an independent estimate of  $f_K/f_\pi$  in isosymmetric QCD with 2+1+1 dynamical flavours of the twisted-mass quarks. Their new set of gauge ensembles reaches the physical pion mass. The quark action includes the Sheikoleslami-Wohlert term [133] for a better control of discretization effects. The finite-volume effects are examined by simulating three spatial volumes, and are corrected by SU(2)  $\chi$ PT formulae [134]. Their new estimate  $f_K/f_\pi = 1.1995(44)_{\text{stat+fit}}(7)_{\text{sys}}$  is consistent with ETM 14E with the total uncertainty reduced by a factor of  $\sim 3.5$ .

FNAL/MILC 17 has determined the ratio of the decay constants from a comprehensive set of HISQ ensembles with  $N_f = 2 + 1 + 1$  dynamical flavours. They have generated 24 ensembles for six values of the lattice spacing (0.03–0.15 fm, scale set with  $f_{\pi^+}$ ) and with both physical and unphysical values of the light sea-quark masses, controlling in

this way the systematic uncertainties due to chiral and continuum extrapolations. With respect to FNAL/MILC 14A they have increased the statistics and added three ensembles at very fine lattice spacings,  $a \simeq 0.03$  and  $0.042$  fm, including for the latter case also a simulation at the physical value of the light-quark mass. The final result of their analysis is  $f_{K^\pm}/f_{\pi^\pm} = 1.1950(14)_{\text{stat}}({}_{-17}^{+0})_{a^2}(2)_{FV}(3)_{f_\pi, PDG}(3)_{EM}(2)_{Q^2}$ , where the errors are statistical, due to the continuum extrapolation, finite-volume, pion decay constant from PDG, electromagnetic effects and sampling of the topological charge distribution.<sup>5</sup>

HPQCD 13A has analyzed ensembles generated by MILC and therefore its study of  $f_{K^\pm}/f_{\pi^\pm}$  is based on the same set of ensembles as FNAL/MILC 17 bar the ones at the finest lattice spacings (namely, only  $a = 0.09$ – $0.15$  fm, scale set with  $f_{\pi^+}$  and relative scale set with the Wilson flow [135, 136]) supplemented by some simulation points with heavier quark masses. HPQCD employs a global fit based on continuum NLO SU(3)  $\chi$ PT for the decay constants supplemented by a model for higher-order terms including discretization and finite-volume effects (61 parameters for 39 data points supplemented by Bayesian priors). Their final result is  $f_{K^\pm}/f_{\pi^\pm} = 1.1916(15)_{\text{stat}}(12)_{a^2}(1)_{FV}(10)$ , where the errors are statistical, due to the continuum extrapolation, due to finite-volume effects and the last error contains the combined uncertainties from the chiral extrapolation, the scale-setting uncertainty, the experimental input in terms of  $f_{\pi^+}$  and from the uncertainty in  $m_u/m_d$ .

Because CalLat 20, FNAL/MILC 17 and HPQCD 13A partly share their gauge ensembles, we assume a 100 % correlation among their statistical errors. A 100 % correlation on the total systematic uncertainty is also assumed between FNAL/MILC 17 and HPQCD 13A with the HISQ valence quarks.

The discretization effects are not large, typically at the  $\lesssim 1$  % level in HPQCD 13A, FNAL/MILC 17 and ETM21 in their simulation region of  $a$ . This does not necessarily mean that  $\delta(a)$  in units of the uncertainty of the observable is small. HPQCD 13A observed that it also depends on the choice of the input to fix the lattice scale:  $\delta(a)$  is consistent with zero with the relative scale setting using  $r_1$  from the static potential and  $w_0$  from the gradient flow, whereas  $\delta(a) \lesssim 7$  with another flow scale  $\sqrt{t_0}$ .<sup>6</sup> It is not surprising that CalLat 20 observed larger scaling violation of  $\lesssim 4$  %: while they partly share gauge ensembles with HPQCD 13A and FNAL/MILC 17, the Möbius domain-wall action without the tree-level  $O(a^2)$  improvement is employed in their mixed action setup.

For  $N_f = 2+1$ , the CLQCD collaboration obtained a new result (CLQCD 23) by employing the tadpole-improved tree-level Symanzik gauge action and tadpole-improved tree-level clover quark action with one-step stout smearing for the gauge link. They simulate three values of the lattice spacing in a wide range  $a = 0.05$ – $0.11$  fm fixed from the gradient-flow scale  $w_0$ . The unitary light-quark mass reaches the physical point on the coarsest lattice. Two additional partially-quenched masses satisfying  $M_\pi L \geq 3.5$  are considered to calculate relevant two-point functions on each ensemble. Their results for  $f_K$  and  $f_\pi$  are renormalized nonperturbatively through the RI/MOM scheme. The chiral extrapolation is based on NLO partially-quenched  $\chi$ PT for  $f_\pi$  and a polynomial form for  $f_K$ . Finite-volume effects are taken into account assuming  $e^{-M_\pi L}$  dependence for data in two volumes on the two coarser lattices. They obtain  $f_{K^\pm}/f_{\pi^\pm} = 1.1907(76)_{\text{stat+fit}}(17)_{\text{sys}}$ , where the second error is taken from the difference with respect to a similar analysis using the RI/SMOM scheme, which shows larger discretization

<sup>5</sup>To form the average in Eq. (76), we have symmetrized the asymmetric systematic error and shifted the central value by half the difference as will be done throughout this section.

<sup>6</sup>We refer to Sec. 11 for detailed discussions on the scale setting and choices of the input.

effects.

The results BMW 16 and QCDSF/UKQCD 16 are also eligible to enter the FLAG average. BMW 16 has analyzed the decay constants evaluated for 47 gauge ensembles generated using tree-level clover-improved fermions with two HEX-smearings and the tree-level Symanzik-improved gauge action. The ensembles correspond to five values of the lattice spacing (0.05–0.12 fm, scale set by  $\Omega$  mass), to pion masses in the range 130–680 MeV and to values of the lattice size from 1.7 to 5.6 fm, obtaining a good control over the interpolation to the physical mass point and the extrapolation to the continuum and infinite volume limits.

QCDSF/UKQCD 16 has used the nonperturbatively  $\mathcal{O}(a)$ -improved clover action for the fermions (mildly stout-smearred) and the tree-level Symanzik action for the gluons. Four values of the lattice spacing (0.06–0.08 fm) have been simulated with pion masses down to  $\sim 220$  MeV and values of the lattice size in the range 2.0–2.8 fm. The decay constants are evaluated using an expansion around the symmetric SU(3) point  $m_u = m_d = m_s = (m_u + m_d + m_s)^{phys}/3$ .

Note, that for  $N_f = 2 + 1$  MILC 10 and HPQCD/UKQCD 07 are based on staggered fermions, BMW 10, BMW 16, QCDSF/UKQCD 16 and CLQCD 23 have used improved Wilson fermions, and RBC/UKQCD 14B's result is based on the domain-wall formulation. In contrast to RBC/UKQCD 14B, BMW 16 and CLQCD 23, the other simulations are for unphysical values of the light-quark masses (corresponding to smallest pion masses in the range 220–260 MeV in the case of MILC 10, HPQCD/UKQCD 07, and QCDSF/UKQCD 16) and, therefore, slightly more sophisticated extrapolations needed to be controlled. Various ansätze for the mass and cutoff dependence comprising SU(2) and SU(3)  $\chi$ PT or simply polynomials were used and compared in order to estimate the model dependence. While BMW 10, RBC/UKQCD 14B, QCDSF/UKQCD 16, and CLQCD 23 are entirely independent computations, subsets of the MILC gauge ensembles used by MILC 10 and HPQCD/UKQCD 07 are the same. MILC 10 is certainly based on a larger and more advanced set of gauge configurations than HPQCD/UKQCD 07. This allows them for a more reliable estimation of gauge systematic effects. In this situation, we consider both statistical and systematic uncertainties to be correlated.

Before determining the average for  $f_{K^\pm}/f_{\pi^\pm}$ , which should be used for applications to Standard Model phenomenology, we apply the strong-isospin correction individually to all those results that have been published only in the isospin-symmetric limit, i.e., BMW 10, HPQCD/UKQCD 07 and RBC/UKQCD 14B at  $N_f = 2 + 1$ . To this end, as in the previous editions of the FLAG reviews [1, 2, 97, 137], we make use of NLO SU(3)  $\chi$ PT [14, 69], which predicts

$$\frac{f_{K^\pm}}{f_{\pi^\pm}} = \frac{f_K}{f_\pi} \sqrt{1 + \delta_{\text{SU}(2)}} , \quad (74)$$

where [14]

$$\delta_{\text{SU}(2)} \approx \sqrt{3} \epsilon_{\text{SU}(2)} \left[ -\frac{4}{3} (f_K/f_\pi - 1) + \frac{2}{3(4\pi)^2 f_0^2} \left( M_K^2 - M_\pi^2 - M_\pi^2 \ln \frac{M_K^2}{M_\pi^2} \right) \right] . \quad (75)$$

We use as input  $\epsilon_{\text{SU}(2)} = \sqrt{3}/(4R)$  with the FLAG result for  $R$  of Eq. (51),  $F_0 = f_0/\sqrt{2} = 80$  (20) MeV,  $M_\pi = 135$  MeV and  $M_K = 495$  MeV (we decided to choose a conservative uncertainty on  $f_0$  in order to reflect the magnitude of potential higher-order corrections). The results are reported in Tab. 18, where in the last column the last error is due to the isospin correction (the remaining errors are quoted in the same order as in the original data).

For  $N_f = 2 + 1 + 1$ , HPQCD [112], FNAL/MILC [108] and ETM [138] estimate a value for  $\delta_{\text{SU}(2)}$  equal to  $-0.0054(14)$ ,  $-0.0052(9)$  and  $-0.0073(6)$ , respectively. Note that the ETM

	$f_K/f_\pi$	$\delta_{\text{SU}(2)}$	$f_{K^\pm}/f_{\pi^\pm}$
HPQCD/UKQCD 07	1.189(2)(7)	-0.0038(6)	1.187(2)(7)(2)
BMW 10	1.192(7)(6)	-0.0039(6)	1.190(7)(6)(2)
RBC/UKQCD 14B	1.1945(45)	-0.0039(6)	1.1921(45)(24)

Table 18: Values of the isospin-breaking correction  $\delta_{\text{SU}(2)}$  applied to the lattice data for  $f_K/f_\pi$ , entering the FLAG average at  $N_f = 2 + 1$ , for obtaining the corrected charged ratio  $f_{K^\pm}/f_{\pi^\pm}$ . The last error in the last column is due to a 100% uncertainty assumed for  $\delta_{\text{SU}(2)}$  from SU(3)  $\chi$ PT.

result is obtained using the insertion of the isovector scalar current according to the expansion method of Ref. [55], while the HPQCD and FNAL/MILC results correspond to the difference between the values of the decay constant ratio extrapolated to the physical  $u$ -quark mass  $m_u$  and to the average  $(m_u + m_d)/2$  light-quark mass.

To remain on the conservative side, we add a 100% error to the correction based on SU(3)  $\chi$ PT. For further analyses, we add (in quadrature) such an uncertainty to the systematic error (see Tab. 18).

Using the results of Tab. 18 for  $N_f = 2 + 1$  we obtain

$$\text{direct, } N_f = 2 + 1 + 1 : f_{K^\pm}/f_{\pi^\pm} = 1.1934(19) \quad \text{Refs. [106–109, 112]}, \quad (76)$$

$$\text{direct, } N_f = 2 + 1 : f_{K^\pm}/f_{\pi^\pm} = 1.1916(34) \quad \text{Refs. [116–118, 120, 123, 126, 131]}, \quad (77)$$

for QCD with broken isospin.

The averages obtained for  $f_+(0)$  and  $f_{K^\pm}/f_{\pi^\pm}$  at  $N_f = 2 + 1$  and  $N_f = 2 + 1 + 1$  [see Eqs. (72–73) and (76–77)] exhibit a precision better than  $\sim 0.3\%$ . At such a level of precision, QED effects cannot be ignored, and a consistent lattice treatment of both QED and QCD effects in leptonic and semileptonic decays becomes mandatory.

### 5.3.3 Extraction of $|V_{ud}|$ and $|V_{us}|$

It is instructive to convert the averages for  $f_+(0)$  and  $f_{K^\pm}/f_{\pi^\pm}$  into a corresponding range for the CKM matrix elements  $|V_{ud}|$  and  $|V_{us}|$ , using the relations in Eq. (65). Consider first the results for  $N_f = 2 + 1 + 1$ . The average for  $f_+(0)$  in Eq. (72) is mapped into the interval  $|V_{us}| = 0.22328(58)$ , depicted as a horizontal red band in Fig. 10. That for  $f_{K^\pm}/f_{\pi^\pm}$  in Eq. (76) is converted into  $|V_{us}|/|V_{ud}| = 0.23126(50)$  using the result for  $|V_{us}/V_{ud}|(f_{K^\pm}/f_{\pi^\pm})$  in Eq. (65), shown as a tilted red band. The red ellipse is the intersection of these two bands and represents the 68% likelihood contour, obtained by treating the above two results as independent measurements. Repeating the exercise for  $N_f = 2 + 1$  leads to the green ellipse.<sup>7</sup> The vertical band shows  $|V_{ud}|$  from nuclear  $\beta$  decay, Eq. (69). The PDG value (69) indicates a tension with both the  $N_f = 2 + 1 + 1$  and  $N_f = 2 + 1$  results from lattice QCD.

As we mentioned, the isospin corrections are becoming relevant for the extraction of the CKM elements at the current precision of lattice QCD inputs. We obtain  $|V_{us}|/|V_{ud}| = 0.23131(45)$  by taking the average of  $f_K/f_\pi$  in isosymmetric QCD and combining it with the

<sup>7</sup>Note that the ellipses shown in Fig. 5 of both Ref. [139] and Ref. [137] correspond instead to the 39% likelihood contours. Note also that in Ref. [137] the likelihood was erroneously stated to be 68% rather than 39%.

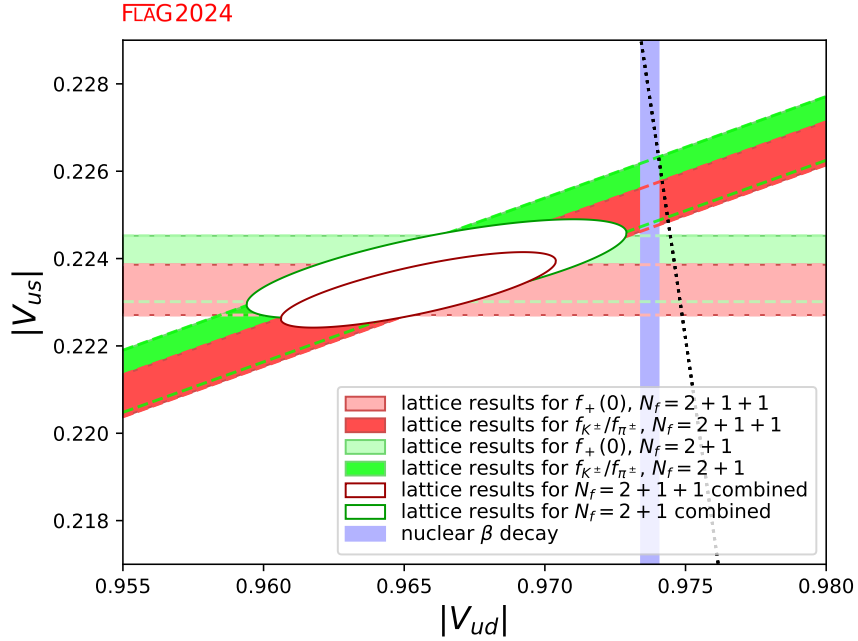


Figure 10: The plot compares the information for  $|V_{ud}|$ ,  $|V_{us}|$  obtained using lattice QCD for  $N_f = 2 + 1$  and  $N_f = 2 + 1 + 1$  with  $|V_{ud}|$  extracted from nuclear  $\beta$  transitions Eq. (69). The black dotted line indicates the correlation between  $|V_{ud}|$  and  $|V_{us}|$  that follows if the CKM-matrix is unitary.

value for  $|V_{us}|f_K/|V_{ud}|f_\pi$  in Eq. (68). This estimate plotted in Fig. 11 is consistent with that obtained from Eq. (65) using the isospin corrections from ChPT. Unlike the corrections from ChPT, the accuracy of the isospin corrections from lattice QCD can be readily improved by more realistic simulations and higher statistics, further sharpening the comparisons shown in the figure.

#### 5.4 Tests of the Standard Model

In the Standard Model, the CKM matrix is unitary. In particular, the elements of the first row obey

$$|V_u|^2 \equiv |V_{ud}|^2 + |V_{us}|^2 + |V_{ub}|^2 = 1. \quad (78)$$

The tiny contribution from  $|V_{ub}|$  is known much better than needed in the present context:  $|V_{ub}| = 3.82(24) \times 10^{-3}$  [4].<sup>8</sup> In the following, we test the first row unitarity Eq. (78) by calculating  $|V_u|^2$  and by analyzing the lattice data within the Standard Model.

In Fig. 10, the correlation between  $|V_{ud}|$  and  $|V_{us}|$  imposed by the unitarity of the CKM matrix is indicated by a dotted line (more precisely, in view of the uncertainty in  $|V_{ub}|$ , the correlation corresponds to a band of finite width, but the effect is too small to be seen here). The plot shows that there is a tension with unitarity in the data for  $N_f = 2 + 1 + 1$ : Numerically, the outcome for the sum of the squares of the first row of the CKM matrix reads

<sup>8</sup>See also Sec. 8.8 for our determination of  $|V_{ub}|$ .

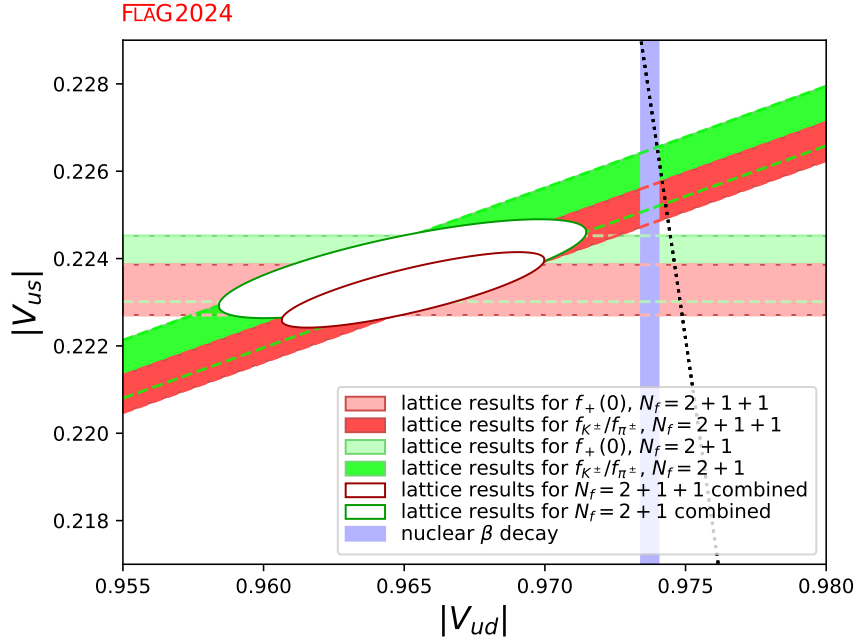


Figure 11: Same as Fig. 10 but with  $|V_{us}|/|V_{ud}|$  obtained using Eq. (68).

$|V_u|^2 = 0.9820(65)$ , which deviates from unity at the level of  $\simeq 2.8$  standard deviations. Still, it is fair to say that at this level the Standard Model passes a nontrivial test on the kaon (semi)leptonic and pion leptonic decays.

The test sharpens considerably by combining the lattice results for  $f_+(0)$  with the  $\beta$  decay value of  $|V_{ud}|$ :  $f_+(0)$  for  $N_f = 2 + 1 + 1$  in Eq. (72) and the PDG estimate of  $|V_{ud}|$  in Eq. (69) lead to  $|V_u|^2 = 0.99802(66)$ , which also shows a  $\simeq 3.0 \sigma$  deviation with unitarity. On the other hand, unitarity is fulfilled ( $1.7 \sigma$ ) with  $f_{K^\pm}/f_{\pi^\pm}$  and  $|V_{ud}|$  (69) ( $|V_u|^2 = 0.99888(67)$ ). Note that the uncertainties on  $|V_u|^2$  coming from the error of  $|V_{ud}|$  is larger by a factor of about three than that from  $|V_{us}|$ .

The situation is similar for  $N_f = 2 + 1$ : with the lattice data alone one has  $|V_u|^2 = 0.9835(89)$ , which is consistent with unity at the level of  $\simeq 1.8$  standard deviations. The lattice results for  $f_+(0)$  in Eqs. (73) with the PDG value of  $|V_{ud}|$  (69) lead to  $|V_u|^2 = 0.99824(69)$ , implying a  $\simeq 2.5 \sigma$  deviation from unitarity, whereas the deviation is reduced to  $1.4 \sigma$  with  $f_{K^\pm}/f_{\pi^\pm}$  in Eq. (77) ( $|V_u|^2 = 0.99903(72)$ ).

## 5.5 Analysis within the Standard Model

The Standard Model implies that the CKM matrix is unitary. The precise experimental constraints quoted in Eq. (65) and the unitarity condition Eq. (78) then reduce the four quantities  $|V_{ud}|, |V_{us}|, f_+(0), f_{K^\pm}/f_{\pi^\pm}$  to a single unknown: any one of these determines the other three within narrow uncertainties.

Numerical results for  $|V_{us}|$  and  $|V_{ud}|$  are listed in Tab. 19, where we restrict ourselves to those determinations that enter the FLAG average in Sec. 5.3 (the error in the experimental

numbers used to convert the values of  $f_+(0)$  and  $f_{K^\pm}/f_{\pi^\pm}$  into values for  $|V_{us}|$  is included in the statistical error). As Fig. 12 shows, the results obtained for  $|V_{us}|$  and  $|V_{ud}|$  from the data on  $f_{K^\pm}/f_{\pi^\pm}$  (squares) are consistent with the determinations via  $f_+(0)$  (triangles), while there is a tendency that  $|V_{us}|$  ( $|V_{ud}|$ ) from  $f_+(0)$  is systematically smaller (larger) than that from  $f_{K^\pm}/f_{\pi^\pm}$ .

Collaboration	Ref.	$N_f$	from	$ V_{us} $	$ V_{ud} $
FNAL/MILC 18	[80]	2 + 1 + 1	$f_+(0)$	0.22333(55)(28)	0.97474(13)(6)
ETM 16	[87]	2 + 1 + 1	$f_+(0)$	0.2230(11)(2)	0.97480(26)(5)
ETM 21	[106]	2 + 1 + 1	$f_{K^\pm}/f_{\pi^\pm}$	0.22490(85)(13)	0.97437(20)(3)
CalLat 20	[107]	2 + 1 + 1	$f_{K^\pm}/f_{\pi^\pm}$	0.22517(65)(56)	0.97431(15)(13)
FNAL/MILC 17	[108]	2 + 1 + 1	$f_{K^\pm}/f_{\pi^\pm}$	0.22513(42)(21)	0.97432(10)(5)
ETM 14E	[109]	2 + 1 + 1	$f_{K^\pm}/f_{\pi^\pm}$	0.2270(22)(20)	0.97388(51)(47)
HPQCD 13A	[112]	2 + 1 + 1	$f_{K^\pm}/f_{\pi^\pm}$	0.22564(42)(29)	0.97420(10)(7)
RBC/UKQCD 15A	[91]	2 + 1	$f_+(0)$	0.22358(89)(32)	0.97468(20)(7)
FNAL/MILC 12I	[71]	2 + 1	$f_+(0)$	0.22400(68)(76)	0.97458(16)(18)
CLQCD 23	[116]	2 + 1	$f_{K^\pm}/f_{\pi^\pm}$	0.2258(14)(3)	0.97417(33)(7)
QCDSF/UKQCD 16	[117]	2 + 1	$f_{K^\pm}/f_{\pi^\pm}$	0.2259(18)(23)	0.97414(42)(54)
BMW 16	[118, 119]	2 + 1	$f_{K^\pm}/f_{\pi^\pm}$	0.2281(19)(48)	0.9736(4)(11)
RBC/UKQCD 14B	[120]	2 + 1	$f_{K^\pm}/f_{\pi^\pm}$	0.22555(87)(43)	0.97422(20)(10)
MILC 10	[123]	2 + 1	$f_{K^\pm}/f_{\pi^\pm}$	0.22503(48)(89)	0.97434(11)(21)
BMW 10	[126]	2 + 1	$f_{K^\pm}/f_{\pi^\pm}$	0.2259(13)(11)	0.97414(30)(26)
HPQCD/UKQCD 07	[131]	2 + 1	$f_{K^\pm}/f_{\pi^\pm}$	0.2265(5)(13)	0.97401(11)(31)

Table 19: Values of  $|V_{us}|$  and  $|V_{ud}|$  obtained from the lattice determinations of either  $f_+(0)$  or  $f_{K^\pm}/f_{\pi^\pm}$  assuming CKM unitarity. The first number in brackets represents the statistical error including the experimental uncertainty, whereas the second is the systematic one.

In order to calculate the average of  $|V_{us}|$  for  $N_f = 2 + 1 + 1$ , we consider the data both for  $f_+(0)$  and  $f_{K^\pm}/f_{\pi^\pm}$ , treating ETM 16 and ETM 14E on the one hand and FNAL/MILC 18, CalLat 20, FNAL/MILC 17, and HPQCD 13A on the other hand, as statistically correlated according to the prescription of Sec. 2.3. We obtain  $|V_{us}| = 0.22483(61)$ , where the error is stretched by a factor  $\sqrt{\chi^2/\text{dof}} \sim \sqrt{2.0}$ . This result is indicated on the left hand side of Fig. 12 by the narrow vertical band. In the case  $N_f = 2 + 1$ , we consider MILC 10, FNAL/MILC 12I and HPQCD/UKQCD 07 on the one hand, and RBC/UKQCD 14B and RBC/UKQCD 15A on the other hand, as mutually statistically correlated, since the analysis in the two cases starts from partially the same set of gauge ensembles. In this way, we arrive at  $|V_{us}| = 0.22490(54)$  with  $\chi^2/\text{dof} \simeq 0.7$ . The figure shows that the results obtained for the data with  $N_f = 2 + 1$  and  $N_f = 2 + 1 + 1$  are consistent with each other. However, the larger error for  $N_f = 2 + 1 + 1$  due to the stretch factor  $\sqrt{\chi^2/\text{dof}}$  suggests a slight tension between the estimates from the semileptonic and leptonic decays.

We take the average of  $|V_{ud}|$  similarly. Again, the result  $|V_{ud}| = 0.97439(14)$  for  $N_f =$



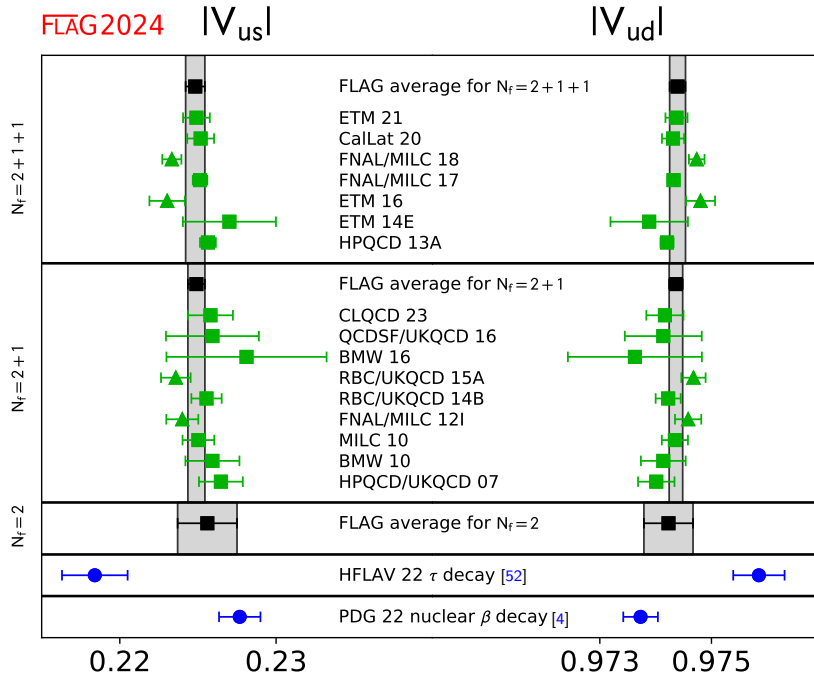


Figure 12: Results for  $|V_{us}|$  and  $|V_{ud}|$  that follow from the lattice data for  $f_+(0)$  (triangles) and  $f_{K^\pm}/f_{\pi^\pm}$  (squares), on the basis of the assumption that the CKM matrix is unitary. The black square and the grey band represent the average for each value of  $N_f$ . For comparison, the figure also indicates the results obtained if the data on nuclear  $\beta$  decay and inclusive hadronic  $\tau$  decay is analyzed within the Standard Model.

$2 + 1 + 1$  is perfectly consistent with the values  $|V_{ud}| = 0.97436(12)$  obtained from the data with  $N_f = 2 + 1$ . These values are consistent with Eq. (69) from the superallowed nuclear transitions within  $2\sigma$ .

As mentioned in Sec. 5.1, the HFLAV value of  $|V_{us}|$  from the inclusive hadronic  $\tau$  decays differs from those obtained from the kaon decays by about three standard deviations. Assuming the first row unitarity defined in Eq. (78) leads to a larger value of  $|V_{ud}|$  than those from the kaon and nuclear decays.

	Ref.	$ V_{us} $	$ V_{ud} $
$N_f = 2 + 1 + 1$		0.22483(61)	0.97439(14)
$N_f = 2 + 1$		0.22490(54)	0.97436(12)
nuclear $\beta$ decay	[4]	0.2277(13)	0.97373(31)
inclusive $\tau$ decay	[52]	0.2184(21)	0.97585(47)

Table 20: The upper half of the table shows the results for  $|V_{us}|$  and  $|V_{ud}|$  from the analysis of the kaon and pion decays within the Standard Model. For comparison, the lower half lists the values that follow if the lattice results are replaced by the experimental results on nuclear  $\beta$  decay and inclusive hadronic  $\tau$  decay, respectively.

## 5.6 Direct determination of $f_{K^\pm}$ and $f_{\pi^\pm}$

It is useful for flavour-physics studies to provide not only the lattice average of  $f_{K^\pm}/f_{\pi^\pm}$ , but also the average of the decay constant  $f_{K^\pm}$ . The case of the decay constant  $f_{\pi^\pm}$  is different, since the the PDG value [7] of this quantity, based on the use of the value of  $|V_{ud}|$  obtained from superallowed nuclear  $\beta$  decays [33], is often used for setting the scale in lattice QCD. However, the physical scale can be set in different ways, namely, by using as input the mass of the  $\Omega$  baryon ( $m_\Omega$ ) or the  $\Upsilon$ -meson spectrum ( $\Delta M_\Upsilon$ ), which are less sensitive to the uncertainties of the chiral extrapolation in the light-quark mass with respect to  $f_{\pi^\pm}$ .<sup>9</sup> In such cases, the value of the decay constant  $f_{\pi^\pm}$  becomes a direct prediction of the lattice-QCD simulations. Therefore, it is interesting to provide also the average of the decay constant  $f_{\pi^\pm}$ , obtained when the physical scale is set through another hadron observable, in order to check the consistency of different scale-setting procedures.

Our compilation of the values of  $f_{\pi^\pm}$  and  $f_{K^\pm}$  with the corresponding colour code is presented in Tab. 21. The new entry in this edition is CLQCD 23 for  $N_f = 2 + 1$ .

In comparison to the case of  $f_{K^\pm}/f_{\pi^\pm}$ , we have added two columns indicating which quantity is used to set the physical scale and the possible use of a renormalization constant for the axial current. For several lattice formulations, the use of the nonsinglet axial-vector Ward identity allows us to avoid the use of any renormalization constant.

One can see that the determinations of  $f_{\pi^\pm}$  and  $f_{K^\pm}$  suffer from larger uncertainties than those of the ratio  $f_{K^\pm}/f_{\pi^\pm}$ , which is less sensitive to various systematic effects (including the uncertainty of a possible renormalization constant) and, moreover, is not exposed to the uncertainties of the procedure used to set the physical scale.

According to the FLAG rules, for  $N_f = 2 + 1 + 1$  four data sets can form the average of  $f_{K^\pm}$  only: ETM 21 [106], ETM 14E [109], FNAL/MILC 14A [110], and HPQCD 13A [112]. Following the same procedure already adopted in Sec. 5.3 for the ratio of the decay constants, we assume 100% statistical and systematic correlation between FNAL/MILC 14A and HPQCD 13A. For  $N_f = 2 + 1$  three data sets can form the average of  $f_{\pi^\pm}$  and  $f_{K^\pm}$ : CLQCD 23 [116], RBC/UKQCD 14B [120] (update of RBC/UKQCD 12), HPQCD/UKQCD 07 [131], and MILC 10 [123], which is the latest update from the MILC program. We consider HPQCD/UKQCD 07 and MILC 10 as statistically and systematically correlated and use the prescription of Sec. 2.3 to form an average.

Thus, our averages read

$$N_f = 2 + 1 : \quad f_{\pi^\pm} = 130.2 (0.8) \text{ MeV} \quad \text{Refs. [116, 120, 123, 131]}, \quad (79)$$

$$N_f = 2 + 1 + 1 : \quad f_{K^\pm} = 155.7 (0.3) \text{ MeV} \quad \text{Refs. [106, 109, 110, 112]}, \quad (80)$$

$$N_f = 2 + 1 : \quad f_{K^\pm} = 155.7 (0.7) \text{ MeV} \quad \text{Refs. [116, 120, 123, 131]}, \quad (81)$$

The lattice results of Tab. 21 and our averages in Eqs. (79)–(81) are reported in Fig. 13. Note that the FLAG average of  $f_{K^\pm}$  for  $N_f = 2 + 1 + 1$  is based on calculations in which  $f_{\pi^\pm}$  is used to set the lattice scale, while the  $N_f = 2 + 1$  average does not rely on that.

<sup>9</sup>See Sec. 11 for detailed discussions.

Collaboration	Ref.	$N_f$	publication status	chiral extrapolation	continuum extrapolation	finite-volume errors	renormalization	physical scale	isospin breaking	$f_{\pi^\pm}$	$f_{K^\pm}$
ETM 21	[106]	2+1+1	A	★	★	★	na	$f_\pi$	–	–	155.92(62)(9) <sup>†</sup>
ETM 14E	[109]	2+1+1	A	○	★	○	na	$f_\pi$	–	–	154.4(1.5)(1.3)
FNAL/MILC 14A	[110]	2+1+1	A	★	★	★	na	$f_\pi$	–	–	155.92(13)( <sup>+34</sup> <sub>-23</sub> )
HPQCD 13A	[112]	2+1+1	A	★	○	★	na	$f_\pi$	–	–	155.37(20)(27)
MILC 13A	[113]	2+1+1	A	★	○	★	na	$f_\pi$	–	–	155.80(34)(54)
ETM 10E	[115]	2+1+1	C	○	○	○	na	$f_\pi$	✓	–	159.6(2.0)
CLQCD 23	[116]	2+1	A	★	○	★	NPR	$w_0$	–	–	130.7(0.9)(2.1)
JLQCD 15C	[140]	2+1	C	○	★	★	NPR	$t_0$	–	–	125.7(7.4) <sub>stat</sub>
RBC/UKQCD 14B	[120]	2+1	A	★	★	★	NPR	$m_\Omega$	✓	–	130.19(89)
RBC/UKQCD 12	[121]	2+1	A	★	○	★	NPR	$m_\Omega$	✓	–	127.1(2.7)(2.7)
Laiho 11	[122]	2+1	C	○	★	○	na	††	–	–	130.53(87)(2.10)
MILC 10	[123]	2+1	C	○	★	★	na	††	–	–	156.8(1.0)(1.7)
MILC 10	[123]	2+1	C	○	★	★	na	$f_\pi$	–	–	129.2(4)(1.4)
JLQCD/TWQCD 10	[124]	2+1	C	○	■	★	na	$m_\Omega$	✓	–	156.1(4)( <sup>+6</sup> <sub>-9</sub> )
RBC/UKQCD 10A	[125]	2+1	A	○	○	★	NPR	$m_\Omega$	✓	–	118.5(3.6) <sub>stat</sub>
MILC 09A	[127]	2+1	C	○	★	★	na	$\Delta M_\Upsilon$	–	–	124(2)(5)
MILC 09A	[127]	2+1	C	○	★	★	na	$f_\pi$	–	–	148.8(2.0)(3.0)
MILC 09	[128]	2+1	A	○	★	★	na	$\Delta M_\Upsilon$	–	–	128.0(0.3)(2.9)
MILC 09	[128]	2+1	A	○	★	★	na	$f_\pi$	–	–	128.3(0.5)( <sup>+2.4</sup> <sub>-3.5</sub> )
MILC 09	[128]	2+1	A	○	★	★	na	$f_\pi$	–	–	154.3(0.4)( <sup>+2.1</sup> <sub>-3.4</sub> )
Aubin 08	[129]	2+1	C	○	○	○	na	$\Delta M_\Upsilon$	–	–	156.5(0.4)( <sup>+1.0</sup> <sub>-2.7</sub> )
RBC/UKQCD 08	[130]	2+1	A	○	■	★	NPR	$m_\Omega$	✓	–	129.1(1.9)(4.0)
HPQCD/UKQCD 07	[131]	2+1	A	○	○	○	na	$\Delta M_\Upsilon$	✓	–	124.1(3.6)(6.9)
MILC 04	[86]	2+1	A	○	○	○	na	$\Delta M_\Upsilon$	–	–	149.4(3.6)(6.3)
											156.7(0.7)(1.9)
											129.5(0.9)(3.5)
											156.6(1.0)(3.6)

The label 'na' indicates the lattice calculations that do not require the use of any renormalization constant for the axial current, while the label 'NPR' signals the use of a renormalization constant calculated nonperturbatively.

<sup>†</sup> We evaluated from  $f_{K^\pm}/f_{\pi^\pm}$  in Tab. 17 and their input to fix the scale  $f_\pi = 130.4(2)$ .

<sup>††</sup> The ratios of lattice spacings within the ensembles were determined using the quantity  $r_1$ . The conversion to physical units was made on the basis of Ref. [141], and we note that such a determination depends on the PDG value [7] of the pion decay constant.

Table 21: Colour codes for the lattice data on  $f_{\pi^\pm}$  and  $f_{K^\pm}$  together with information on the way the lattice spacing was converted to physical units and on whether or not an isospin-breaking correction has been applied to the quoted result (see Sec. 5.3). The numerical values are listed in MeV units. In this and previous editions [1, 97], old results with two red tags have been dropped.

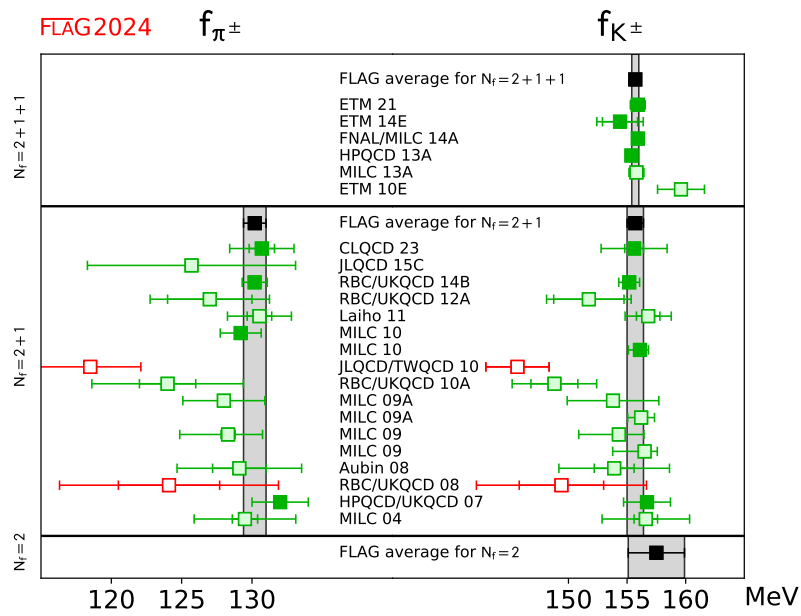


Figure 13: Values of  $f_{\pi^\pm}$  and  $f_{K^\pm}$ . The black squares and grey bands indicate our averages in Eqs. (79) and (81).

## References

- [1] [FLAG 21] Y. Aoki et al., *FLAG Review 2021*, *Eur. Phys. J. C* **82** (2022) 869 [[2111.09849](#)].
- [2] [FLAG 16] S. Aoki et al., *Review of lattice results concerning low-energy particle physics*, *Eur. Phys. J.* **C77** (2017) 112 [[1607.00299](#)].
- [3] M. Moulson, *Experimental determination of  $V_{us}$  from kaon decays*, *PoS CKM2016* (2017) 033 [[1704.04104](#)].
- [4] PARTICLE DATA GROUP collaboration, *Review of Particle Physics*, *PTEP* **2022** (2022) 083C01.
- [5] J. Gasser and G.R.S. Zarnauskas, *On the pion decay constant*, *Phys. Lett.* **B693** (2010) 122 [[1008.3479](#)].
- [6] PARTICLE DATA GROUP collaboration, *Review of Particle Physics*, *Chin. Phys.* **C38** (2014) 090001 and 2015 update.
- [7] PARTICLE DATA GROUP collaboration, *Review of Particle Physics*, *Chin. Phys.* **C40** (2016) 100001.
- [8] J. Gasser, A. Rusetsky and I. Scimemi, *Electromagnetic corrections in hadronic processes*, *Eur. Phys. J.* **C32** (2003) 97 [[hep-ph/0305260](#)].
- [9] A. Rusetsky, *Isospin symmetry breaking*, *PoS* **CD09** (2009) 071 [[0910.5151](#)].
- [10] J. Gasser, *Theoretical progress on cusp effect and  $K_{\ell 4}$  decays*, *PoS* **KAON07** (2008) 033 [[0710.3048](#)].
- [11] V. Cirigliano, M. Knecht, H. Neufeld, H. Rupertsberger and P. Talavera, *Radiative corrections to  $K(l3)$  decays*, *Eur. Phys. J. C* **23** (2002) 121 [[hep-ph/0110153](#)].
- [12] V. Cirigliano, H. Neufeld and H. Pichl,  *$K(e3)$  decays and CKM unitarity*, *Eur. Phys. J. C* **35** (2004) 53 [[hep-ph/0401173](#)].
- [13] V. Cirigliano, M. Giannotti and H. Neufeld, *Electromagnetic effects in  $K(l3)$  decays*, *JHEP* **11** (2008) 006 [[0807.4507](#)].
- [14] V. Cirigliano and H. Neufeld, *A note on isospin violation in  $P_{\ell 2}(\gamma)$  decays*, *Phys.Lett.* **B700** (2011) 7 [[1102.0563](#)].
- [15] N. Carrasco, V. Lubicz, G. Martinelli, C.T. Sachrajda, N. Tantalo, C. Tarantino et al., *QED Corrections to Hadronic Processes in Lattice QCD*, *Phys. Rev.* **D91** (2015) 074506 [[1502.00257](#)].
- [16] D. Giusti, V. Lubicz, G. Martinelli, C.T. Sachrajda, F. Sanfilippo, S. Simula et al., *First lattice calculation of the QED corrections to leptonic decay rates*, *Phys. Rev. Lett.* **120** (2018) 072001 [[1711.06537](#)].

- [17] M. Di Carlo, D. Giusti, V. Lubicz, G. Martinelli, C. Sachrajda, F. Sanfilippo et al., *Light-meson leptonic decay rates in lattice QCD+QED*, *Phys. Rev. D* **100** (2019) 034514 [[1904.08731](#)].
- [18] J.L. Rosner, S. Stone and R.S. Van de Water, *Leptonic Decays of Charged Pseudoscalar Mesons*, in *Review of Particle Physics [6] 2015 update*, [1509.02220](#).
- [19] P. Boyle et al., *Isospin-breaking corrections to light-meson leptonic decays from lattice simulations at physical quark masses*, *JHEP* **02** (2023) 242 [[2211.12865](#)].
- [20] N. Hermansson-Truedsson, M. Di Carlo, M.T. Hansen and A. Portelli, *Structure-dependent electromagnetic finite-volume effects through order  $1/L^3$* , *PoS LATTICE2023* (2024) 265 [[2310.13358](#)].
- [21] C.Y. Seng, M. Gorchtein and M.J. Ramsey-Musolf, *Dispersive evaluation of the inner radiative correction in neutron and nuclear  $\beta$  decay*, *Phys. Rev. D* **100** (2019) 013001 [[1812.03352](#)].
- [22] C.-Y. Seng, M. Gorchtein, H.H. Patel and M.J. Ramsey-Musolf, *Reduced hadronic uncertainty in the determination of  $V_{ud}$* , *Phys. Rev. Lett.* **121** (2018) 241804 [[1807.10197](#)].
- [23] W.J. Marciano and A. Sirlin, *Improved calculation of electroweak radiative corrections and the value of  $V(ud)$* , *Phys. Rev. Lett.* **96** (2006) 032002 [[hep-ph/0510099](#)].
- [24] A. Czarnecki, W.J. Marciano and A. Sirlin, *Radiative Corrections to Neutron and Nuclear Beta Decays Revisited*, *Phys. Rev. D* **100** (2019) 073008 [[1907.06737](#)].
- [25] P.-X. Ma, X. Feng, M. Gorchtein, L.-C. Jin, K.-F. Liu, C.-Y. Seng et al., *Lattice QCD Calculation of Electroweak Box Contributions to Superallowed Nuclear and Neutron Beta Decays*, *Phys. Rev. Lett.* **132** (2024) 191901 [[2308.16755](#)].
- [26] I.S. Towner and J.C. Hardy, *An improved calculation of the isospin-symmetry-breaking corrections to superallowed Fermi  $\beta$  decay*, *Phys. Rev.* **C77** (2008) 025501 [[0710.3181](#)].
- [27] G.A. Miller and A. Schwenk, *Isospin-symmetry-breaking corrections to superallowed Fermi  $\beta$  decay: formalism and schematic models*, *Phys. Rev.* **C78** (2008) 035501 [[0805.0603](#)].
- [28] N. Auerbach, *Coulomb corrections to superallowed  $\beta$  decay in nuclei*, *Phys. Rev.* **C79** (2009) 035502 [[0811.4742](#)].
- [29] H. Liang, N. Van Giai and J. Meng, *Isospin corrections for superallowed Fermi  $\beta$  decay in self-consistent relativistic random-phase approximation approaches*, *Phys. Rev.* **C79** (2009) 064316 [[0904.3673](#)].
- [30] G.A. Miller and A. Schwenk, *Isospin-symmetry-breaking corrections to superallowed Fermi  $\beta$  decay: radial excitations*, *Phys. Rev.* **C80** (2009) 064319 [[0910.2790](#)].
- [31] I. Towner and J. Hardy, *Comparative tests of isospin-symmetry-breaking corrections to superallowed  $0^+ \rightarrow 0^+$  nuclear  $\beta$  decay*, *Phys.Rev.* **C82** (2010) 065501 [[1007.5343](#)].

- [32] J.C. Hardy and I.S. Towner, *Superaligned  $0^+ \rightarrow 0^+$  nuclear  $\beta$  decays: 2014 critical survey, with precise results for  $V_{ud}$  and CKM unitarity*, *Phys. Rev.* **C91** (2015) 025501 [[1411.5987](#)].
- [33] J. Hardy and I.S. Towner,  $|V_{ud}|$  from nuclear  $\beta$  decays, *PoS CKM2016* (2016) 028.
- [34] M. Gorchtein,  $\gamma W$  Box Inside Out: Nuclear Polarizabilities Distort the Beta Decay Spectrum, *Phys. Rev. Lett.* **123** (2019) 042503 [[1812.04229](#)].
- [35] J.C. Hardy and I.S. Towner, *Superaligned  $0^+ \rightarrow 0^+$  nuclear  $\beta$  decays: 2020 critical survey, with implications for  $V_{ud}$  and CKM unitarity*, *Phys. Rev. C* **102** (2020) 045501.
- [36] E. Gamiz, M. Jamin, A. Pich, J. Prades and F. Schwab, *Determination of  $m_s$  and  $|V_{us}|$  from hadronic  $\tau$  decays*, *JHEP* **01** (2003) 060 [[hep-ph/0212230](#)].
- [37] E. Gamiz, M. Jamin, A. Pich, J. Prades and F. Schwab,  $V_{us}$  and  $m_s$  from hadronic  $\tau$  decays, *Phys. Rev. Lett.* **94** (2005) 011803 [[hep-ph/0408044](#)].
- [38] K. Maltman, *A mixed  $\tau$ -electroproduction sum rule for  $V_{us}$* , *Phys. Lett.* **B672** (2009) 257 [[0811.1590](#)].
- [39] A. Pich and R. Kass, *talks given at CKM 2008*, <http://ckm2008.roma1.infn.it>.
- [40] E. Gamiz, M. Jamin, A. Pich, J. Prades and F. Schwab, *Theoretical progress on the  $V_{us}$  determination from  $\tau$  decays*, *PoS KAON07* (2008) 008 [[0709.0282](#)].
- [41] E. Gamiz,  $|V_{us}|$  from hadronic  $\tau$  decays, *CKM 2012*, [1301.2206](#).
- [42] K. Maltman, C. E. Wolfe, S. Banerjee, J. M. Roney and I. Nugent, *Status of the hadronic  $\tau$  determination of  $V_{us}$* , *Int. J. Mod. Phys.* **A23** (2008) 3191 [[0807.3195](#)].
- [43] K. Maltman, C. E. Wolfe, S. Banerjee, I. M. Nugent and J. M. Roney, *Status of the hadronic  $\tau$  decay determination of  $|V_{us}|$* , *Nucl. Phys. Proc. Suppl.* **189** (2009) 175 [[0906.1386](#)].
- [44] [HFLAV 18] Y. Amhis et al., *Averages of  $b$ -hadron,  $c$ -hadron, and  $\tau$ -lepton properties as of 2018*, *Eur. Phys. J. C* **81** (2021) 226 [[1909.12524](#)].
- [45] K. Maltman, P. Boyle, R. Hudspith, T. Izubuchi, A. Jüttner, C. Lehner et al., *Current Status of inclusive hadronic tau determinations of  $|V_{us}|$* , *SciPost Phys. Proc.* (2019) 6.
- [46] [RBC/UKQCD 18] P. Boyle, R.J. Hudspith, T. Izubuchi, A. Jüttner, C. Lehner, R. Lewis et al., *Novel  $|V_{us}|$  Determination Using Inclusive Strange  $\tau$  Decay and Lattice Hadronic Vacuum Polarization Functions*, *Phys. Rev. Lett.* **121** (2018) 202003 [[1803.07228](#)].
- [47] A. Crivellin, M. Kirk, T. Kitahara and F. Mescia, *Global fit of modified quark couplings to EW gauge bosons and vector-like quarks in light of the Cabibbo angle anomaly*, *JHEP* **03** (2023) 234 [[2212.06862](#)].
- [48] M.T. Hansen, H.B. Meyer and D. Robaina, *From deep inelastic scattering to heavy-flavor semileptonic decays: Total rates into multihadron final states from lattice QCD*, *Phys. Rev. D* **96** (2017) 094513 [[1704.08993](#)].

- [49] P. Gambino and S. Hashimoto, *Inclusive Semileptonic Decays from Lattice QCD*, *Phys. Rev. Lett.* **125** (2020) 032001 [[2005.13730](#)].
- [50] [ETM 23A] A. Evangelista, R. Frezzotti, N. Tantalo, G. Gagliardi, F. Sanfilippo, S. Simula et al., *Inclusive hadronic decay rate of the  $\tau$  lepton from lattice QCD*, *Phys. Rev. D* **108** (2023) 074513 [[2308.03125](#)].
- [51] [ETM 24] C. Alexandrou et al., *Inclusive hadronic decay rate of the  $\tau$  lepton from lattice QCD: the  $\bar{u}s$  flavour channel and the Cabibbo angle*, *Phys. Rev. Lett.* **132** (2024) 261901 [[2403.05404](#)].
- [52] HFLAV collaboration, *Averages of  $b$ -hadron,  $c$ -hadron, and  $\tau$ -lepton properties as of 2021*, *Phys. Rev. D* **107** (2023) 052008 [[2206.07501](#)].
- [53] M. Antonelli et al., *An evaluation of  $|V_{us}|$  and precise tests of the Standard Model from world data on leptonic and semileptonic kaon decays*, *Eur. Phys. J. C* **69** (2010) 399 [[1005.2323](#)].
- [54] [PACS-CS 08] S. Aoki et al., *2+1 flavor lattice QCD toward the physical point*, *Phys. Rev. D* **79** (2009) 034503 [[0807.1661](#)].
- [55] [RM123 11] G. M. de Divitiis, P. Dimopoulos, R. Frezzotti, V. Lubicz, G. Martinelli et al., *Isospin breaking effects due to the up-down mass difference in lattice QCD*, *JHEP* **1204** (2012) 124 [[1110.6294](#)].
- [56] T. Ishikawa, T. Blum, M. Hayakawa, T. Izubuchi, C. Jung et al., *Full QED+QCD low-energy constants through reweighting*, *Phys.Rev.Lett.* **109** (2012) 072002 [[1202.6018](#)].
- [57] T. Izubuchi, *Lattice QCD + QED - from Isospin breaking to  $g-2$  light-by-light*, talk given at Lattice 2012, Cairns, Australia, <http://www.physics.adelaide.edu.au/cssm/lattice2012>.
- [58] [RM123 13] G. M. de Divitiis, R. Frezzotti, V. Lubicz, G. Martinelli, R. Petronzio et al., *Leading isospin breaking effects on the lattice*, *Phys.Rev.* **D87** (2013) 114505 [[1303.4896](#)].
- [59] N. Tantalo, *Isospin Breaking Effects on the Lattice*, *PoS LATTICE2013* (2014) 007 [[1311.2797](#)].
- [60] A. Portelli, *Inclusion of isospin breaking effects in lattice simulations*, *PoS LATTICE2014* (2015) 013 [[1505.07057](#)].
- [61] N.H. Christ, X. Feng, L.-C. Jin, C.T. Sachrajda and T. Wang, *Radiative corrections to leptonic decays using infinite-volume reconstruction*, *Phys. Rev. D* **108** (2023) 014501 [[2304.08026](#)].
- [62] N.H. Christ, X. Feng, L. Jin, C.T. Sachrajda and T. Wang, *Lattice Calculation of Electromagnetic Corrections to  $Kl3$  decay*, *PoS LATTICE2023* (2024) 266 [[2402.08915](#)].
- [63] C.-Y. Seng, X. Feng, M. Gorchtein, L.-C. Jin and U.-G. Meißner, *New method for calculating electromagnetic effects in semileptonic beta-decays of mesons*, *JHEP* **10** (2020) 179 [[2009.00459](#)].



- [64] P.-X. Ma, X. Feng, M. Gorchtein, L.-C. Jin and C.-Y. Seng, *Lattice QCD calculation of the electroweak box diagrams for the kaon semileptonic decays*, *Phys. Rev. D* **103** (2021) 114503 [2102.12048].
- [65] C.-Y. Seng, D. Galviz, M. Gorchtein and U.-G. Meißner, *Improved  $K_{e3}$  radiative corrections sharpen the  $K_{\mu 2}$ - $K_{l3}$  discrepancy*, *JHEP* **11** (2021) 172 [2103.04843].
- [66] M. Ademollo and R. Gatto, *Nonrenormalization theorem for the strangeness violating vector currents*, *Phys. Rev. Lett.* **13** (1964) 264.
- [67] J. Gasser and H. Leutwyler, *Low-energy expansion of meson form factors*, *Nucl. Phys.* **B250** (1985) 517.
- [68] G. Furlan, F. Lannoy, C. Rossetti and G. Segré, *Symmetry-breaking corrections to weak vector currents*, *Nuovo Cim.* **38** (1965) 1747.
- [69] J. Gasser and H. Leutwyler, *Chiral perturbation theory: expansions in the mass of the strange quark*, *Nucl. Phys.* **B250** (1985) 465.
- [70] C. Bernard, J. Bijnens and E. Gamiz, *Semileptonic kaon decay in staggered chiral perturbation theory*, *Phys. Rev.* **D89** (2014) 054510 [1311.7511].
- [71] [FNAL/MILC 12I] A. Bazavov, C. Bernard, C. Bouchard, C. DeTar, D. Du et al., *Kaon semileptonic vector form factor and determination of  $|V_{us}|$  using staggered fermions*, *Phys.Rev.* **D87** (2013) 073012 [1212.4993].
- [72] [RBC 08A] J. M. Flynn and C.T. Sachrajda,  *$SU(2)$  chiral perturbation theory for  $K_{\ell 3}$  decay amplitudes*, *Nucl. Phys.* **B812** (2009) 64 [0809.1229].
- [73] H. Leutwyler and M. Roos, *Determination of the elements  $V_{us}$  and  $V_{ud}$  of the Kobayashi-Maskawa matrix*, *Z. Phys.* **C25** (1984) 91.
- [74] P. Post and K. Schilcher,  *$K_{l3}$  form factors at order  $p^6$  in chiral perturbation theory*, *Eur. Phys. J.* **C25** (2002) 427 [hep-ph/0112352].
- [75] J. Bijnens and P. Talavera,  *$K_{l3}$  decays in chiral perturbation theory*, *Nucl. Phys.* **B669** (2003) 341 [hep-ph/0303103].
- [76] M. Jamin, J.A. Oller and A. Pich, *Order  $p^6$  chiral couplings from the scalar  $K\pi$  form factor*, *JHEP* **02** (2004) 047 [hep-ph/0401080].
- [77] V. Cirigliano et al., *The Green function and  $SU(3)$  breaking in  $K_{l3}$  decays*, *JHEP* **04** (2005) 006 [hep-ph/0503108].
- [78] A. Kastner and H. Neufeld, *The  $K_{l3}$  scalar form factors in the Standard Model*, *Eur. Phys. J.* **C57** (2008) 541 [0805.2222].
- [79] [JLQCD 17] S. Aoki, G. Cossu, X. Feng, H. Fukaya, S. Hashimoto, T. Kaneko et al., *Chiral behavior of  $K \rightarrow \pi l \nu$  decay form factors in lattice QCD with exact chiral symmetry*, *Phys. Rev.* **D96** (2017) 034501 [1705.00884].
- [80] [FNAL/MILC 18] A. Bazavov et al.,  *$|V_{us}|$  from  $K_{\ell 3}$  decay and four-flavor lattice QCD*, *Phys. Rev.* **D99** (2019) 114509 [1809.02827].

- [81] V. Bernard and E. Passemar, *Matching chiral perturbation theory and the dispersive representation of the scalar  $K\pi$  form-factor*, *Phys. Lett.* **B661** (2008) 95 [[0711.3450](#)].
- [82] A. Duncan, E. Eichten and H. Thacker, *Electromagnetic splittings and light quark masses in lattice QCD*, *Phys. Rev. Lett.* **76** (1996) 3894 [[hep-lat/9602005](#)].
- [83] [MILC 08] S. Basak et al., *Electromagnetic splittings of hadrons from improved staggered quarks in full QCD*, *PoS LAT2008* (2008) 127 [[0812.4486](#)].
- [84] T. Blum et al., *Electromagnetic mass splittings of the low lying hadrons and quark masses from 2+1 flavor lattice QCD+QED*, *Phys. Rev.* **D82** (2010) 094508 [[1006.1311](#)].
- [85] [BMW 10C] A. Portelli et al., *Electromagnetic corrections to light hadron masses*, *PoS LAT2010* (2010) 121 [[1011.4189](#)].
- [86] [MILC 04] C. Aubin et al., *Light pseudoscalar decay constants, quark masses and low energy constants from three-flavor lattice QCD*, *Phys. Rev.* **D70** (2004) 114501 [[hep-lat/0407028](#)].
- [87] [ETM 16] N. Carrasco, P. Lami, V. Lubicz, L. Riggio, S. Simula and C. Tarantino,  *$K \rightarrow \pi$  semileptonic form factors with  $N_f = 2 + 1 + 1$  twisted mass fermions*, *Phys. Rev.* **D93** (2016) 114512 [[1602.04113](#)].
- [88] [FNAL/MILC 13E] A. Bazavov et al., *Determination of  $|V_{us}|$  from a lattice-QCD calculation of the  $K \rightarrow \pi\ell\nu$  semileptonic form factor with physical quark masses*, *Phys. Rev. Lett.* **112** (2014) 112001 [[1312.1228](#)].
- [89] [PACS 22] K.-I. Ishikawa, N. Ishizuka, Y. Kuramashi, Y. Namekawa, Y. Taniguchi, N. Ukita et al.,  *$K\ell 3$  form factors at the physical point: Toward the continuum limit*, *Phys. Rev. D* **106** (2022) 094501 [[2206.08654](#)].
- [90] [PACS 19] J. Kakazu, K.-i. Ishikawa, N. Ishizuka, Y. Kuramashi, Y. Nakamura, Y. Namekawa et al.,  *$K_{l3}$  form factors at the physical point on  $(10.9\text{ fm})^3$  volume*, *Phys. Rev. D* **101** (2020) 094504 [[1912.13127](#)].
- [91] [RBC/UKQCD 15A] P.A. Boyle et al., *The kaon semileptonic form factor in  $N_f = 2 + 1$  domain wall lattice QCD with physical light quark masses*, *JHEP* **1506** (2015) 164 [[1504.01692](#)].
- [92] [RBC/UKQCD 13] P. A. Boyle, J.M. Flynn, N. Garron, A. Jüttner, C.T. Sachrajda et al., *The kaon semileptonic form factor with near physical domain wall quarks*, *JHEP* **1308** (2013) 132 [[1305.7217](#)].
- [93] [JLQCD 12] T. Kaneko et al., *Chiral behavior of kaon semileptonic form factors in lattice QCD with exact chiral symmetry*, *PoS LAT2012* (2012) 111 [[1211.6180](#)].
- [94] [JLQCD 11] T. Kaneko et al., *Kaon semileptonic form factors in QCD with exact chiral symmetry*, *PoS LAT2011* (2011) 284 [[1112.5259](#)].
- [95] [RBC/UKQCD 10] P. A. Boyle et al.,  *$K \rightarrow \pi$  form factors with reduced model dependence*, *Eur.Phys.J.* **C69** (2010) 159 [[1004.0886](#)].

- [96] [RBC/UKQCD 07] P. A. Boyle, A. Jüttner, R. Kenway, C. Sachrajda, S. Sasaki et al.,  $K_{13}$  semileptonic form-factor from 2+1 flavour lattice QCD, *Phys.Rev.Lett.* **100** (2008) 141601 [0710.5136].
- [97] [FLAG 19] S. Aoki et al., *FLAG Review 2019: Flavour Lattice Averaging Group (FLAG)*, *Eur. Phys. J. C* **80** (2020) 113 [1902.08191].
- [98] D. Guadagnoli, F. Mescia and S. Simula, *Lattice study of semileptonic form-factors with twisted boundary conditions*, *Phys.Rev.* **D73** (2006) 114504 [hep-lat/0512020].
- [99] [UKQCD 07] P. A. Boyle, J. Flynn, A. Jüttner, C. Sachrajda and J. Zanotti, *Hadronic form factors in lattice QCD at small and vanishing momentum transfer*, *JHEP* **0705** (2007) 016 [hep-lat/0703005].
- [100] [ETM 10J] V. Lubicz, F. Mescia, L. Orifici, S. Simula and C. Tarantino, *Improved analysis of the scalar and vector form factors of kaon semileptonic decays with  $N_f = 2$  twisted-mass fermions*, *PoS LATTICE2010* (2010) 316 [1012.3573].
- [101] [SPQcdR 04] D. Bećirević et al., *The  $K \rightarrow \pi$  vector form factor at zero momentum transfer on the lattice*, *Nucl. Phys.* **B705** (2005) 339 [hep-ph/0403217].
- [102] [ETM 09K] V. Lubicz, F. Mescia, S. Simula and C. Tarantino,  *$K \rightarrow \pi l \nu$  Semileptonic Form Factors from Two-Flavor Lattice QCD*, *Phys. Rev. D* **80** (2009) 111502 [0906.4728].
- [103] C. Bernard, J. Bijnens, E. Gámiz and J. Relefors, *Twisted finite-volume corrections to  $K_{13}$  decays with partially-quenched and rooted-staggered quarks*, *JHEP* **03** (2017) 120 [1702.03416].
- [104] [PACS 23A] T. Yamazaki, K.-i. Ishikawa, N. Ishizuka, Y. Kuramashi, Y. Namekawa, Y. Taniguchi et al.,  $|V_{us}|$  from kaon semileptonic form factor in  $N_f = 2 + 1$  QCD at the physical point on  $(10 \text{ fm})^4$ , *PoS LATTICE2023* (2024) 276 [2311.16755].
- [105] G. Amoros, J. Bijnens and P. Talavera, *QCD isospin breaking in meson masses, decay constants and quark mass ratios*, *Nucl. Phys.* **B602** (2001) 87 [hep-ph/0101127].
- [106] [ETM 21] C. Alexandrou et al., *Ratio of kaon and pion leptonic decay constants with  $N_f = 2 + 1 + 1$  Wilson-clover twisted-mass fermions*, *Phys. Rev. D* **104** (2021) 074520 [2104.06747].
- [107] [CalLat 20] N. Miller et al.,  $f_K/f_\pi$  from Möbius domain-wall fermions solved on gradient-flowed hisq ensembles, *Phys. Rev. D* **102** (2020) 034507 [2005.04795].
- [108] [FNAL/MILC 17] A. Bazavov et al.,  *$B$ - and  $D$ -meson leptonic decay constants from four-flavor lattice QCD*, *Phys. Rev.* **D98** (2018) 074512 [1712.09262].
- [109] [ETM 14E] N. Carrasco, P. Dimopoulos, R. Frezzotti, P. Lami, V. Lubicz et al., *Leptonic decay constants  $f_K$ ,  $f_D$  and  $f_{D_s}$  with  $N_f = 2+1+1$  twisted-mass lattice QCD*, *Phys.Rev.* **D91** (2015) 054507 [1411.7908].
- [110] [FNAL/MILC 14A] A. Bazavov et al., *Charmed and light pseudoscalar meson decay constants from four-flavor lattice QCD with physical light quarks*, *Phys.Rev.* **D90** (2014) 074509 [1407.3772].

- [111] [ETM 13F] P. Dimopoulos, R. Frezzotti, P. Lami, V. Lubicz, E. Picca et al., *Pseudoscalar decay constants  $f_K/f_\pi$ ,  $f_D$  and  $f_{D_s}$  with  $N_f = 2 + 1 + 1$  ETMC configurations*, *PoS LATTICE2013* (2014) 314 [[1311.3080](#)].
- [112] [HPQCD 13A] R. Dowdall, C. Davies, G. Lepage and C. McNeile,  *$V_{us}$  from  $\pi$  and  $K$  decay constants in full lattice QCD with physical  $u$ ,  $d$ ,  $s$  and  $c$  quarks*, *Phys.Rev.* **D88** (2013) 074504 [[1303.1670](#)].
- [113] [MILC 13A] A. Bazavov, C. Bernard, C. DeTar, J. Foley, W. Freeman et al., *Leptonic decay-constant ratio  $f_{K^+}/f_{\pi^+}$  from lattice QCD with physical light quarks*, *Phys.Rev.Lett.* **110** (2013) 172003 [[1301.5855](#)].
- [114] [MILC 11] A. Bazavov et al., *Properties of light pseudoscalars from lattice QCD with HISQ ensembles*, *PoS LAT2011* (2011) 107 [[1111.4314](#)].
- [115] [ETM 10E] F. Farchioni, G. Herdoiza, K. Jansen, M. Petschlies, C. Urbach et al., *Pseudoscalar decay constants from  $N_f = 2 + 1 + 1$  twisted mass lattice QCD*, *PoS LAT2010* (2010) 128 [[1012.0200](#)].
- [116] [CLQCD 23] Zhi-Cheng Hu et al., *Quark masses and low-energy constants in the continuum from the tadpole-improved clover ensembles*, *Phys. Rev. D* **109** (2024) 054507 [[2310.00814](#)].
- [117] [QCDSF/UKQCD 16] V. G. Bornyakov, R. Horsley, Y. Nakamura, H. Perlt, D. Pleiter, P.E.L. Rakow et al., *Flavour breaking effects in the pseudoscalar meson decay constants*, *Phys. Lett.* **B767** (2017) 366 [[1612.04798](#)].
- [118] [BMW 16] S. Dürr et al., *Leptonic decay-constant ratio  $f_K/f_\pi$  from lattice QCD using 2+1 clover-improved fermion flavors with 2-HEX smearing*, *Phys. Rev.* **D95** (2017) 054513 [[1601.05998](#)].
- [119] E.E. Scholz and S. Dürr, *Leptonic decay-constant ratio  $f_K/f_\pi$  from clover-improved  $N_f = 2 + 1$  QCD*, *PoS LATTICE2016* (2016) 283 [[1610.00932](#)].
- [120] [RBC/UKQCD 14B] T. Blum et al., *Domain wall QCD with physical quark masses*, *Phys. Rev.* **D93** (2016) 074505 [[1411.7017](#)].
- [121] [RBC/UKQCD 12] R. Arthur et al., *Domain wall QCD with near-physical pions*, *Phys.Rev.* **D87** (2013) 094514 [[1208.4412](#)].
- [122] J. Laiho and R.S. Van de Water, *Pseudoscalar decay constants, light-quark masses and  $B_K$  from mixed-action lattice QCD*, *PoS LATTICE2011* (2011) 293 [[1112.4861](#)].
- [123] [MILC 10] A. Bazavov et al., *Results for light pseudoscalar mesons*, *PoS LAT2010* (2010) 074 [[1012.0868](#)].
- [124] [JLQCD/TWQCD 10] J. Noaki et al., *Chiral properties of light mesons in  $N_f = 2 + 1$  overlap QCD*, *PoS LAT2010* (2010) 117.
- [125] [RBC/UKQCD 10A] Y. Aoki et al., *Continuum limit physics from 2+1 flavor domain wall QCD*, *Phys.Rev.* **D83** (2011) 074508 [[1011.0892](#)].

- [126] [BMW 10] S. Dürr, Z. Fodor, C. Hoelbling, S. Katz, S. Krieg et al., *The ratio  $F_K/F_\pi$  in QCD*, *Phys.Rev.* **D81** (2010) 054507 [[1001.4692](#)].
- [127] [MILC 09A] A. Bazavov et al., *MILC results for light pseudoscalars*, *PoS* **CD09** (2009) 007 [[0910.2966](#)].
- [128] [MILC 09] A. Bazavov et al., *Full nonperturbative QCD simulations with 2+1 flavors of improved staggered quarks*, *Rev. Mod. Phys.* **82** (2010) 1349 [[0903.3598](#)].
- [129] C. Aubin, J. Laiho and R.S. Van de Water, *Light pseudoscalar meson masses and decay constants from mixed action lattice QCD*, *PoS* **LAT2008** (2008) 105 [[0810.4328](#)].
- [130] [RBC/UKQCD 08] C. Allton et al., *Physical results from 2+1 flavor domain wall QCD and  $SU(2)$  chiral perturbation theory*, *Phys. Rev.* **D78** (2008) 114509 [[0804.0473](#)].
- [131] [HPQCD/UKQCD 07] E. Follana, C.T.H. Davies, G.P. Lepage and J. Shigemitsu, *High precision determination of the  $\pi$ ,  $K$ ,  $D$  and  $D_s$  decay constants from lattice QCD*, *Phys. Rev. Lett.* **100** (2008) 062002 [[0706.1726](#)].
- [132] B. Ananthanarayan, J. Bijnens, S. Friot and S. Ghosh, *Analytic representation of  $f_K/f_\pi$  in two loop chiral perturbation theory*, *Physical Review D* **97** (2018) .
- [133] B. Sheikholeslami and R. Wohlert, *Improved continuum limit lattice action for QCD with Wilson fermions*, *Nucl. Phys.* **B259** (1985) 572.
- [134] G. Colangelo, S. Dürr and C. Haefeli, *Finite volume effects for meson masses and decay constants*, *Nucl. Phys.* **B721** (2005) 136 [[hep-lat/0503014](#)].
- [135] M. Lüscher, *Properties and uses of the Wilson flow in lattice QCD*, *JHEP* **08** (2010) 071 [[1006.4518](#)], [Erratum: *JHEP* **03** (2014) 092].
- [136] [BMW 12A] S. Borsanyi, S. Dürr, Z. Fodor, C. Hoelbling, S.D. Katz et al., *High-precision scale setting in lattice QCD*, *JHEP* **1209** (2012) 010 [[1203.4469](#)].
- [137] [FLAG 13] S. Aoki, Y. Aoki, C. Bernard, T. Blum, G. Colangelo et al., *Review of lattice results concerning low-energy particle physics*, *Eur.Phys.J.* **C74** (2014) 2890 [[1310.8555](#)].
- [138] D. Giusti, V. Lubicz, G. Martinelli, F. Sanfilippo, S. Simula, N. Tantalo et al., *Leading isospin-breaking corrections to meson masses on the lattice*, *EPJ Web Conf.* **175** (2018) 06002 [[1710.06633](#)].
- [139] [FLAG 10] G. Colangelo, S. Dürr, A. Jüttner, L. Lellouch, H. Leutwyler et al., *Review of lattice results concerning low energy particle physics*, *Eur.Phys.J.* **C71** (2011) 1695 [[1011.4408](#)].
- [140] [JLQCD 15C] B. Fahy, G. Cossu, S. Hashimoto, T. Kaneko, J. Noaki and M. Tomii, *Decay constants and spectroscopy of mesons in lattice QCD using domain-wall fermions*, *PoS* **LATTICE2015** (2016) 074 [[1512.08599](#)].
- [141] [HPQCD 09B] C. T. H. Davies, E. Follana, I. Kendall, G.P. Lepage and C. McNeile, *Precise determination of the lattice spacing in full lattice QCD*, *Phys.Rev.* **D81** (2010) 034506 [[0910.1229](#)].